

Electronic Theses and Dissertations, 2004-2019

2013

The Contribution Of Visceral Fat To Positive Insulin Signaling In Ames Dwarf Mice

Vinal Menon
University of Central Florida

 Part of the [Biotechnology Commons](#), and the [Molecular Biology Commons](#)
Find similar works at: <https://stars.library.ucf.edu/etd>
University of Central Florida Libraries <http://library.ucf.edu>

This Masters Thesis (Open Access) is brought to you for free and open access by STARS. It has been accepted for inclusion in Electronic Theses and Dissertations, 2004-2019 by an authorized administrator of STARS. For more information, please contact STARS@ucf.edu.

STARS Citation

Menon, Vinal, "The Contribution Of Visceral Fat To Positive Insulin Signaling In Ames Dwarf Mice" (2013). *Electronic Theses and Dissertations, 2004-2019*. 2662.
<https://stars.library.ucf.edu/etd/2662>

THE CONTRIBUTION OF VISCERAL FAT TO POSITIVE INSULIN SIGNALING IN
AMES DWARF MICE

by

VINAL VINOD MENON

Master of Technology (Biotechnology), Padmashree Dr. D. Y. Patil University, Mumbai, India,
2010

A thesis submitted in partial fulfillment of the requirements
for the degree of Master of Science
in the Department of Biotechnology
in the Burnett School of Biomedical Sciences,
in the College of Medicine
at the University of Central Florida
Orlando, Florida

Summer Term
2013

Major Professor: Michal M. Masternak

© 2013 Vinal Vinod Menon

ABSTRACT

Ames dwarf (df/df) mice are homozygous for a spontaneous mutation in the *prop1* gene due to which there is no development of anterior pituitary cells – somatotrophs, lactotrophs and thyrotrophs, leading to a deficiency of growth hormone (GH), prolactin (PRL) and thyrotropin (TSH). They tend to become obese as they age, but still live longer and healthier lives compared to their wild-type littermates, being very insulin sensitive, showing no signs of diabetes and cancer. These mutant mice also have high circulating levels of anti-inflammatory and anti-diabetic adiponectin. Plasma levels of this adipokine usually decrease with an increase in accumulation of visceral fat (VF). We thus believe that VF in df/df mice, developed in the absence of GH signaling, may be functionally different from the same fat depots in normal (N) mice and may be beneficial, rather than detrimental, to the overall health of the animal. We performed surgeries involving removal of VF depots (epididymal and perirenal fat) in both groups of mice and hypothesize that the beneficial effects of visceral fat removal (VFR) will be present exclusively in N mice as VF in df/df mice contributes to enhanced insulin sensitivity by producing decreased levels of pro-inflammatory adipokines like TNF α and IL-6. We found that VFR improved insulin sensitivity only in N mice but not in the df/df mice. This intervention led to an upregulation of certain players of the insulin signaling pathway in the skeletal muscle of N mice only, with no alteration in df/df mice. The subcutaneous fat of df/df mice showed a downregulation of these insulin signaling genes upon VFR. Compared to N mice, epididymal fat of df/df mice (sham-operated) had increased gene expression of some of the players involved in insulin signaling and a decrease in transcript levels of TNF α . Ames dwarf mice had decreased levels of IL-6 protein in EF and in circulation. High circulating levels of adiponectin and

decreased levels of IL-6 in circulation could contribute to the high insulin sensitivity observed in the Ames dwarf mice. Understanding the mechanisms responsible for VF having positive effects on insulin signaling in df/df mice would be important for future treatment of obese diabetic patients.

ACKNOWLEDGMENTS

It is with a deep sense of gratitude and fulfillment that I acknowledge the encouragement and inspiration I have received from the University of Central Florida biomedical science faculty, the various departmental teams, and support groups:

Dr. Michal Masternak, Principal Investigator and Committee Chair, for his patient and attentive mentorship, inspiring me to pursue excellence at every stage, and taking me to this point of academic and research accomplishment.

Dr. Deborah Altomare, Dr. Alvaro Estevez and Dr. Annette Khaled, committee members, for their reassurance, motivation and guidance throughout my research endeavor.

Dr. Xu Zhi, Dr. Tanvir Hossain, Dr. Adam Gesing, Denise Wiesenborn and Andrew Do, lab members, who were always forthcoming in their support, giving direction to my research efforts.

Teresa Krisch, Rashell Hallford and James Grant, UCF vivarium staff, who constantly proved to be a caring team, forever helpful.

Dr. Andrzej Bartke and Adam Spong, collaborators at Southern Illinois University, School of Medicine, for their valuable contributions.

Veethika Pandey and Lina Spinel, members of Dr. Altomare's Lab, who readily offered assistance at various stages.

Lisa Vaughn, Judith Ramos and Lisa Simcoe, administrative staff, for their cooperative spirit, always ready to help.

My parents, who taught me to be passionate and sincere in everything I do.

This study was supported by the National Institute on Aging of the National Institutes of Health under award number RO1AG032290

TABLE OF CONTENTS

LIST OF FIGURES	x
LIST OF TABLES	xii
CHAPTER 1: INTRODUCTION	1
1.1 The Ames dwarf mouse	1
1.2 Adipose tissue	3
1.3 Visceral fat vs. subcutaneous fat.....	4
1.4 Calorie restriction.....	5
1.5 Visceral fat removal	5
1.6 Fat as an endocrine organ	7
1.7 Obesity, inflammation and diabetes.....	9
1.8 The insulin signaling pathway	13
1.9 Growth hormone, insulin sensitivity and longevity	16
CHAPTER 2: MATERIALS AND METHODS	20
2.1 Experimental animals.....	20
2.2 Visceral fat removal (VFR)	20
2.3 Fat adiponectin and serum IL-6 levels.....	21
2.4 Analysis of glucose tolerance and whole-body insulin sensitivity	21
2.5 Insulin stimulation and tissue collection.....	22

2.6 RNA extraction from frozen tissue	22
2.7 cDNA synthesis	23
2.8 Quantitative real-time polymerase chain reaction (qPCR)	26
2.9 Protein extraction from frozen tissue	29
2.10 Western blotting.....	29
2.11 Enzyme-linked immunosorbent assay (ELISA) for adiponectin (plasma)	30
2.12 Enzyme-linked immunosorbent assay (ELISA) for adiponectin (adipose tissue)	31
2.13 Enzyme-linked immunosorbent assay (ELISA) for insulin (plasma).....	31
2.14 Bio-Plex Pro™ Assay for IL-6 levels in serum	31
CHAPTER 3 RESULTS	33
3.1 Body weight and visceral fat content.....	33
3.2 Whole-body insulin sensitivity	35
3.3 Effect of VFR on expression of insulin signaling genes in skeletal muscle.....	38
3.4 Effect of VFR on the phosphorylation state of Akt in skeletal muscle	40
3.5 Effect of VFR on expression of insulin signaling genes in subcutaneous fat.....	43
3.6 Local expression of IGF-1 in different tissues of the Ames dwarf mouse	46
3.7 Differential gene expression levels in epididymal fat could contribute to enhanced insulin sensitivity in Ames dwarf mice.....	48
3.8 Adiponectin and IL-6 protein levels in the Ames dwarf mouse	50

CHAPTER 4: DISCUSSION.....	52
REFERENCES	60

LIST OF FIGURES

Figure 1: Extended longevity of Ames dwarf compared to normal mice.....	2
Figure 2: Adipose tissue depots of an adult Sv129 mouse.	3
Figure 3: Various factors secreted by white adipose tissue	7
Figure 4: Metabolic processes regulated by AMPK.....	9
Figure 5: Immune cell types in adipose tissue under lean and obese conditions.....	10
Figure 6: The insulin signaling pathway.....	14
Figure 7: Mutations in growth-promoting pathways extend longevity and are conserved from yeast to mammals.....	16
Figure 8: Decreased longevity of df/df mice upon early-life GH treatment.....	19
Figure 9: Effect of VFR on body weight of df/df and N mice.....	33
Figure 10: Visceral fat content (absolute and percentage of body weight) of N and df/df mice.	34
Figure 11: Glucose tolerance test (GTT) and insulin tolerance test (ITT)	35
Figure 12: Effect of VFR on fasting blood glucose levels.....	36
Figure 13: Plasma insulin levels and HOMA score.....	37
Figure 14: Differential gene expression upon VFR in skeletal muscle of N and df/df mice.....	39
Figure 15: Expression of total Akt protein in skeletal muscle.....	40
Figure 16: Effect of VFR on phosphorylation levels of Akt in skeletal muscle.....	42
Figure 17: Effect of VFR on gene expression in subcutaneous fat.....	44
Figure 18: Local expression of IGF-1 in different tissues of df/df mice	46
Figure 19: Increased expression of genes promoting insulin sensitivity in epididymal fat of Ames dwarf mice	48

Figure 20: Ames dwarf mice show a downregulation in the expression of TNF α transcript in epididymal fat 49

Figure 21: Adiponectin levels in circulation and in different fat pads 50

Figure 22: IL-6 protein levels in EF and serum..... 51

Figure 23: Proposed mechanisms of extended longevity in df/df mice..... 58

LIST OF TABLES

Table 1: cDNA synthesis using iScript™ cDNA Synthesis Kit (Bio-Rad).....	24
Table 2: Run protocol for iScript™ cDNA Synthesis Kit (Bio-Rad).....	24
Table 3: cDNA synthesis using EasyScript Plus™ cDNA synthesis kit (Applied Biological Materials)	25
Table 4: Run protocol for cDNA synthesis with EasyScript Plus™ cDNA synthesis kit (Applied Biological Materials)	25
Table 5: qPCR reaction mix components	26
Table 6: Primer sequences for qPCR	27

CHAPTER 1: INTRODUCTION

1.1 The Ames dwarf mouse

Discovered in one of the mouse colonies at Iowa State University, Ames dwarf (df/df) mice are homozygous for a spontaneous mutation in the *Prophet of pituitary factor-1 (Prop1)* gene whose product is responsible for pituitary development. Due to the loss-of-function mutation, the df/df mice are devoid of three anterior pituitary cell types – somatotrophs, lactotrophs and thyrotrophs – resulting in these mutants being deficient in the hormones secreted by these cells – growth hormone (GH), prolactin (PRL) and thyrotropin (TSH). Though indistinguishable from their siblings at birth, adult df/df mice are one-third the size of their normal (N) littermates. These mutant mice are very insulin sensitive, having low circulating levels of insulin and glucose. Due to GH deficiency, circulating levels of insulin-like growth factor 1 (IGF-1) are significantly low in the df/df mice. These mice tend to get obese as they age. However, they still maintain high circulating adiponectin levels. Calorie restriction (CR) is a dietary intervention that is known to extend longevity and increase healthspan in rodents. However, through a single genetic mutation, df/df mice live significantly longer and healthier lives compared to N mice (figure 1) [1-3]. The difference in average lifespan between df/df and N mice was more than 350 days for males and more than 470 days for females [1]. Protection from developing age-related disorders may contribute to the enhanced lifespan and healthspan of these mutant dwarf mice. In addition to maintaining their youthful appearance with age, Ames dwarf mice do not show a decline in locomotor activity that is normally seen in aging mice; old mutants are much more active than the younger Ames dwarf mice [4]. Also, these mutants do not show an age-related decline in memory [4] and are less prone to cancer [5]. Even though df/df

mice share some characteristics of N mice on CR, which include small body size, decreased body temperature and low plasma levels of glucose, insulin and IGF-1, they are not CR mimetics. In fact, CR further extends the lifespan of df/df mice [6].

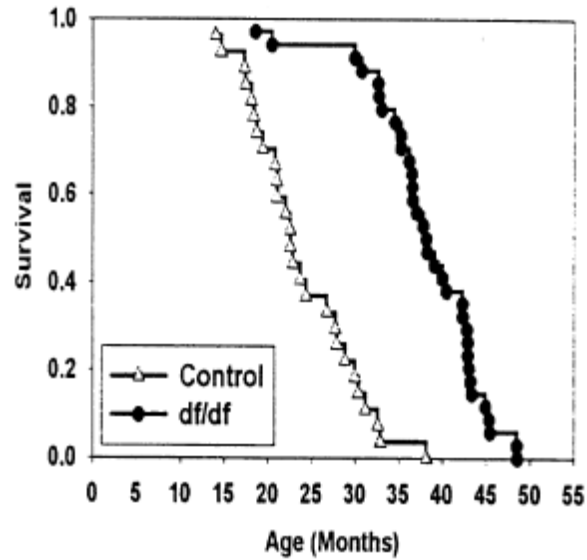


Figure 1: Extended longevity of Ames dwarf compared to normal mice
(Bartke A, B.-B.H., Mattison J, Kinney B, Hauck S, Wright C., *Prolonged longevity of hypopituitary dwarf mice*. *Exp Gerontol*, 2001. 36(1): p. 21-8)

1.2 Adipose tissue

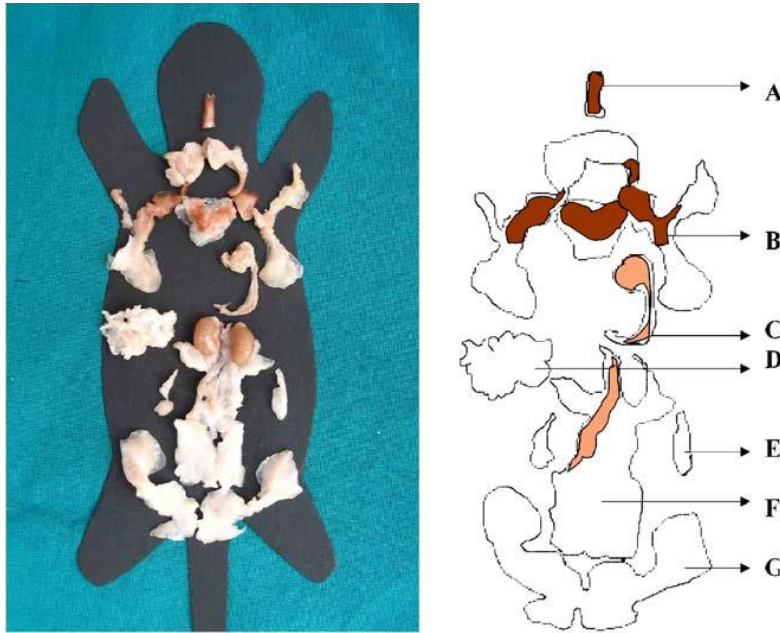


Figure 2: Adipose tissue depots of an adult Sv129 mouse.

A → deep cervical, B → anterior subcutaneous (interscapular, subscapular, axillo-toracic, superficial cervical), C → visceral mediastinic, D → visceral mesenteric, E → visceral retroperitoneal, F → visceral perirenal, periovaric, para- metrial and perivescical, G → posterior subcutaneous (dorso-lumbar, inguinal and gluteal)

(S, C., *The adipose organ*. Prostaglandins Leukot Essent Fatty Acids, 2005. 73(1): p. 9-15)

Mammals have two distinct types of adipose tissue – white and brown. White adipose tissue (WAT) serves as a fat-storing organ. It secretes several biologically active peptides that control whole-body insulin sensitivity. WAT also functions to provide thermal insulation and protects other organs from mechanical damage. Fat cells (adipocytes) in brown adipose tissue (BAT) have a large number of mitochondria and express uncoupling protein1 (UCP1), which leads to heat production via mitochondrial uncoupling of oxidative phosphorylation.

Thus, BAT is involved in non-shivering thermogenesis [7]; but it also exhibits anti-obesity and anti-diabetic properties [8]. Our study focuses exclusively on the role of WAT, located in the visceral cavity, on insulin signaling in *df/df* mice.

1.3 Visceral fat vs. subcutaneous fat

Subcutaneous (SQ) fat refers to adipose tissue located beneath the skin. In mice, the main regions of accumulation of visceral fat (VF) are around the kidney – the perirenal (PR) fat depot – and around the gonads – epididymal fat (EF) in males. The site of vascular drainage from adipose tissue can affect insulin sensitivity and glucose tolerance. SQ fat blood drains into systemic circulation. However, due to the location of VF in the body, the liver has direct access to free fatty acids and pro-inflammatory adipokines, such as TNF α and IL-6, released by these depots via portal circulation, contributing to systemic inflammation and insulin resistance in obese mice as well as humans [9, 10].

The size of adipocytes also contributes to insulin sensitivity. Small adipocytes, as found in SQ fat, are insulin sensitive. However, VF has a greater population of larger insulin-resistant adipocytes [11].

There have been several studies on laboratory animals showing that surgical removal of visceral fat improves insulin sensitivity and glucose tolerance (as detailed below). Moreover, transplanting SQ fat from donor mice into the visceral cavity of recipient mice had the most beneficial effects on whole-body insulin sensitivity and glucose tolerance compared to other fat transplantation combinations [12]. These studies strengthen the idea that SQ is ‘good’ fat whereas VF represents ‘bad’ body fat.

1.4 Calorie restriction

Calorie restriction (CR), a decrease in the intake of calories without leading to malnutrition, is known to prevent or reverse many diseases associated with aging, including obesity and diabetes. CR leads to significant increases in longevity in many species including mice and rats [13]. The most striking responses to CR in mammals are a decrease in insulin levels, an increase in insulin sensitivity [14] and a loss of fat mass [15]. Ames dwarf mice exhibit several characteristics shown by wild-type mice on CR. However, the mutant dwarfs tend to get obese as they age; but they still benefit from the effects of CR [6].

1.5 Visceral fat removal

Several groups have carried out surgical removal of VF depots in different animal models, as well as in humans, to address the association of VF with insulin resistance. Removal of epididymal and perinephric fat pads from Sprague-Dawley rats led to an improvement in hepatic insulin sensitivity and also a decrease in the expression of TNF α in subcutaneous fat [16]. Another study involving monosodium glutamate-obese (MSG-Ob) rats showed that visceral fat (epididymal and retroperitoneal fat) removal normalized the level of plasma free fatty acids (FFA) and hepatic glucose production (HGP) rate. However, removal of subcutaneous fat resulted only in partial normalization of the plasma level of FFA but HGP was not significantly decreased compared to control mice [17]. This study showed that visceral fat has more effect on liver insulin sensitivity and FFA concentration than does subcutaneous fat. The natural process of aging involves an accumulation of visceral fat, which could be a potential causative factor for insulin resistance. Removal of visceral fat

from aging rats improved peripheral and hepatic insulin sensitivity [18]. Omentectomy – removal of the omentum and associated fat – in dogs provided further evidence that extracting a small amount of visceral fat can significantly improve insulin sensitivity [19].

Benefits of VF removal in human subjects have been conflicting. Various studies have been undertaken to prove or disprove the addition of omentectomy to other bariatric surgery procedures. One pilot study has revealed that combining omentectomy and adjustable gastric banding could result in beneficial, long-term effects on the metabolic profile in obese patients [20]. However, a study by Csendes et al compared laparotomic resectional gastric bypass alone and in combination with omentectomy [21]. They reported that there was no difference between the two groups, two years after surgery, with respect to blood sugar levels, serum insulin and other parameters. They concluded that omentectomy is not justified as part of bariatric surgery. Furthermore, another study showed that omentectomy did not enhance the improvement in hepatic or peripheral insulin sensitivity in obese patients who underwent Roux-en-Y gastric bypass surgery, and also did not improve insulin sensitivity, glucose effectiveness and β -cell function in obese diabetic patients [22]. It was thus inferred that an increase in visceral fat is not a major cause of metabolic dysfunction. Hirashita et al compared visceral fat resection and gastric banding in obese diabetic rats [23]. They showed that visceral fat removal decreased the levels of glucose and insulin. This procedure also increased plasma adiponectin levels and decreased circulating TNF α levels. However, gastric banding had better effects on glucose, insulin adiponectin, TNF α and insulin sensitivity compared to visceral fat resection. This study concluded that removal of visceral fat did have a small effect on improving insulin sensitivity and glucose tolerance, in comparison to gastric

banding. Thus, combining the two procedures did not have any additional benefit on insulin sensitivity and glucose tolerance. Further testing has to be carried out to justify the addition of VF removal to current bariatric surgery procedures.

1.6 Fat as an endocrine organ

Previously thought to be just a passive storage organ, it is now well accepted that adipose tissue functions as an endocrine organ, secreting several biologically active peptides (figure 3) known as adipokines which include adiponectin, TNF α and IL-6 [24].

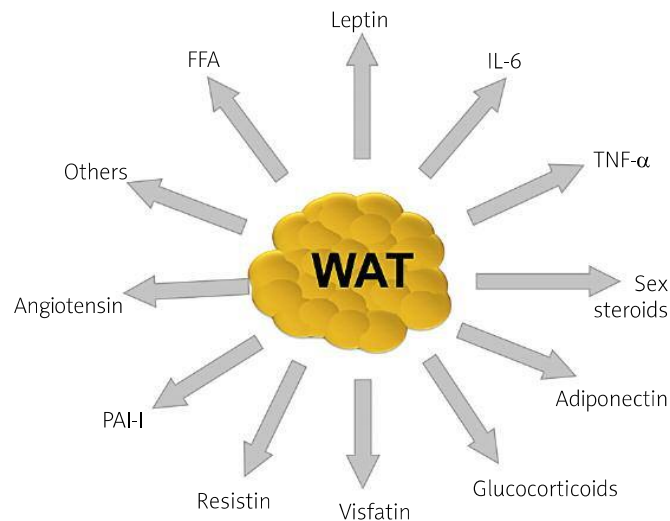


Figure 3: Various factors secreted by white adipose tissue

(Coelho M, O.T., Fernandes R, *Biochemistry of adipose tissue: an endocrine organ*. Arch Med Sci, 2013. 9(2): p. 191-200)

The expression of adiponectin decreases with an increase in obesity [25-27] while that of pro-inflammatory adipokines including TNF α and IL-6, increases with the accumulation of

visceral fat [28]. Conversely, weight loss results in an increase in the plasma levels of adiponectin [29-31] and a decrease in circulating levels of TNF α and IL-6 [32].

Adiponectin exhibits anti-diabetic properties, sensitizing the body to the actions of insulin. It enhances insulin signaling by decreasing triglyceride levels in skeletal muscle. This adipokine signals through the AMP-activated protein kinase (AMPK) pathway (figure 4) leading to increased fatty acid oxidation and glucose uptake in myocytes and a decrease in the expression of enzymes involved in gluconeogenesis in the liver, thus lowering blood glucose levels [33]. In addition to its insulin-sensitizing effects, adiponectin also has anti-inflammatory functions; it inhibits the expression of endothelial adhesion molecules and proliferation of vascular smooth muscle cells. Adiponectin also blocks the formation of foam cells and induces the production of anti-inflammatory IL-10 [34]. The fact that adiponectin is indeed a beneficial adipokine was strengthened by experiments involving the injections of this hormone into obese, insulin-resistant mice leading to an improvement in insulin sensitivity [35, 36].

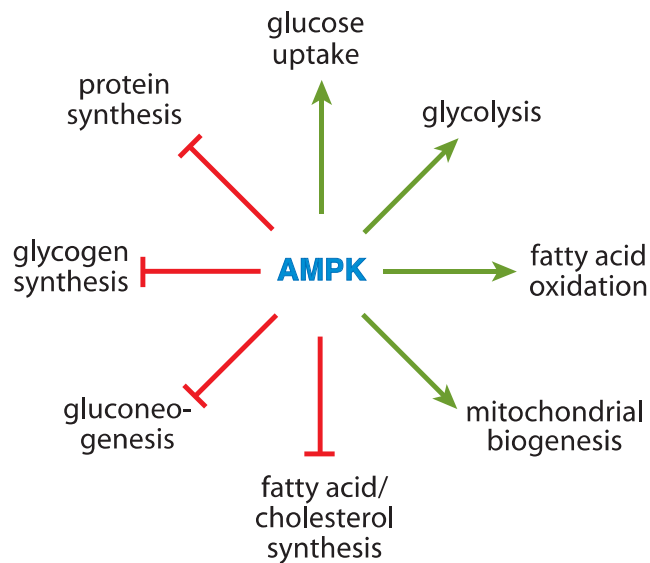


Figure 4: Metabolic processes regulated by AMPK

(Green → activation; red → inhibition)

(Hardie DG, H.S., Scott JW, AMP-activated protein kinase--development of the energy sensor concept. J Physiol, 2006. 574(Pt 1): p. 1-15)

Interleukin-6 stimulates the release of CRP from the liver. TNF α terminates insulin signal transduction by serine-phosphorylation of insulin receptor substrate-1 (IRS-1) thus preventing its association with the β subunit of the insulin receptor leading to insulin resistance [34].

1.7 Obesity, inflammation and diabetes

Obesity is a serious medical condition, especially prevalent in developed countries. It was recently reported that more than 35% adults and around 17% children and adolescents in the United States are obese [37]. This state of excess fat accumulation results when there is an

imbalance between energy intake and expenditure. An increase in the consumption of larger portions of unhealthy foods and a relative decrease in physical activity are the major causes contributing to obesity [38, 39].

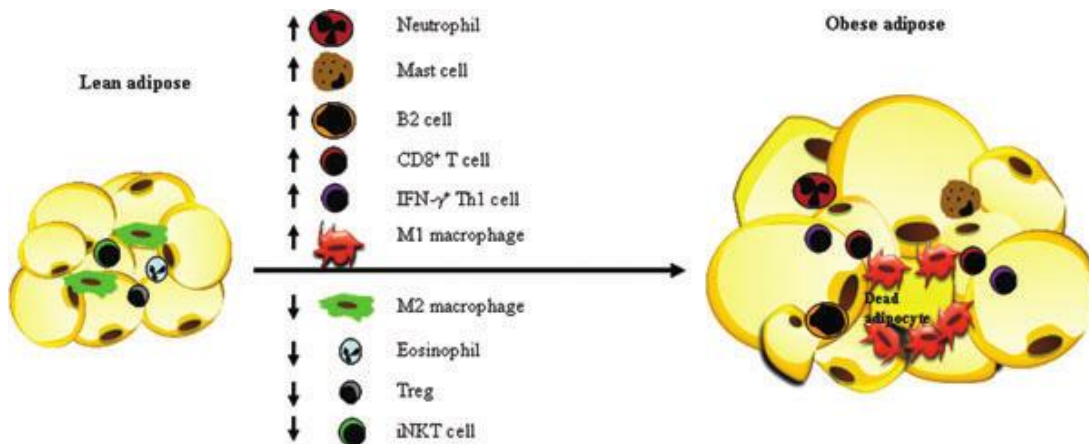


Figure 5: Immune cell types in adipose tissue under lean and obese conditions
 (Feng B, Z.T., Xu H, *Human adipose dynamics and metabolic health*. Ann N Y Acad Sci, 2013. 1281:
 p. 160-77)

The shift in the secretion of adipokines during obesity, with the release of more pro-inflammatory adipokines such as TNF α and IL-6 and a decrease in the release of anti-inflammatory adiponectin, leads to a chronic state of low-grade systemic inflammation. Visceral fat in obese subjects is infiltrated with a large number of macrophages (figure 5) [40]. The expression of another adipokine, monocyte chemoattractant protein-1 (MCP-1), is also increased in obesity [41], leading to a greater recruitment of circulating monocytes. Transgenic mice overexpressing MCP-1 showed an increase in the influx of macrophages into adipose tissue while mice with a targeted disruption of the MCP-1 gene showed reduced infiltration of

macrophages into adipose tissue [42]. This establishes the fact that MCP-1 plays an important role in the recruitment of macrophages into visceral adipose depots. Monocytes that are recruited into adipose tissue then differentiate into mature macrophages under the action of colony stimulating factor 1 (CSF1), also produced by adipocytes [34]. Importantly, macrophages also infiltrate adipose tissue depots in non-obese conditions. However, these are of the M2 (alternatively activated) phenotype and thus provide protection from inflammation. In the setting of obesity, there is a switch from M2 to M1 (classically activated) macrophages thus contributing to the inflammatory state [43]. Interestingly, it was shown that the switch results from the recruitment of circulating macrophages of the pro-inflammatory phenotype into clusters and not just a conversion of resident M2 cells to the M1 phenotype in adipose tissue [44].

Diabetes, as characterized primarily by hyperglycemia, could be due to autoimmune destruction of the pancreatic β -cells (Type 1 diabetes) or due to target organs becoming resistant to the actions of insulin (Type 2 diabetes) [45]. Only 5% of diabetic patients suffer from the type 1 form of the disease, making type 2 diabetes the most common form of this disorder, which is now being diagnosed across all ages and in both genders. According to the American Diabetes Association (ADA), 25.8 million people (8.3% of the population) in the United States have diabetes. Type 2 diabetes is most often associated with obesity and physical inactivity. If untreated, this disease could lead to several medical complications including heart disease, renal failure, blindness and even death [45]. Insulin resistance, associated with obesity and diabetes, involves insulin-target organs – adipose tissue, skeletal muscle and liver – being non-responsive to the actions of insulin. There is a decrease in insulin-stimulated glucose uptake in fat and muscle cells and reduced suppression of intrinsic glucose production by the liver [46]. As stated

above, visceral fat accumulation leads to a state of inflammation via secretion of pro-inflammatory cytokines such as IL-6 and TNF α . Also, the high rate of lipolysis leads to increased portal drainage of free fatty acids into the liver. These events hamper the insulin signaling pathway in the target organs leading to insulin resistance [47]. The body responds to elevated glucose levels by increased pancreatic secretion of insulin. However, chronic hyperglycemia leads to a decrease in the secretion of insulin over time due to destruction of the β -cells.

Treating diabetes and its associated medical complications is expensive not only for patients but also for national healthcare systems. Patients suffering from diabetes may even need hospitalization for treatment of diabetes-related conditions such as heart/kidney damage, blindness and limb amputation, leading to increased expenses [48]. The ADA reports a 41% increase in costs over a five-year period – up from \$174 billion in 2007 to \$245 billion in 2012. Developing therapeutic interventions for obesity, insulin resistance and diabetes is not only expensive but also a time-consuming process, which pharmaceutical companies are now focusing on due to the increasing number of obese diabetics. Moreover, many such drugs, approved by the FDA, have adverse side effects. One such example is the class of drugs known as thiazolidinediones (TZD), used in the treatment of type 2 diabetes. They act via peroxisome proliferator-activated receptor gamma (PPAR γ) to improve whole-body insulin sensitivity [49]. However, the use of these drugs have been associated with edema and heart failure [50], increased osteoporosis [51] and hepatotoxicity [52].

The study carried out here throws light on the fact that visceral fat in df/df mice differs from the same fat depots in N mice and does not negatively affect insulin sensitivity in these

mutant dwarfs. Understanding the mechanisms that underlie this differential function would be important for development of new therapeutic strategies to treat obese diabetic patients. Such therapies would involve manipulating the endocrine organ to improve insulin sensitivity at the whole-body level; and due to the target specificity would avoid any adverse side effects.

1.8 The insulin signaling pathway

Insulin is a hormone released by the pancreatic β cells and is involved in regulating blood glucose levels. It increases glucose disposal in skeletal muscle and adipose tissue by stimulating the translocation of the GLUT4 glucose transporter from its intracellular location to the plasma membrane and blocks intrinsic hepatic glucose production (gluconeogenesis) by inhibiting the activity of gluconeogenic enzymes. An excess of fat (obesity) as well as loss of fat (lipoatrophy) can lead to insulin resistance further emphasizing the role of fat in maintaining whole-body insulin sensitivity [53].

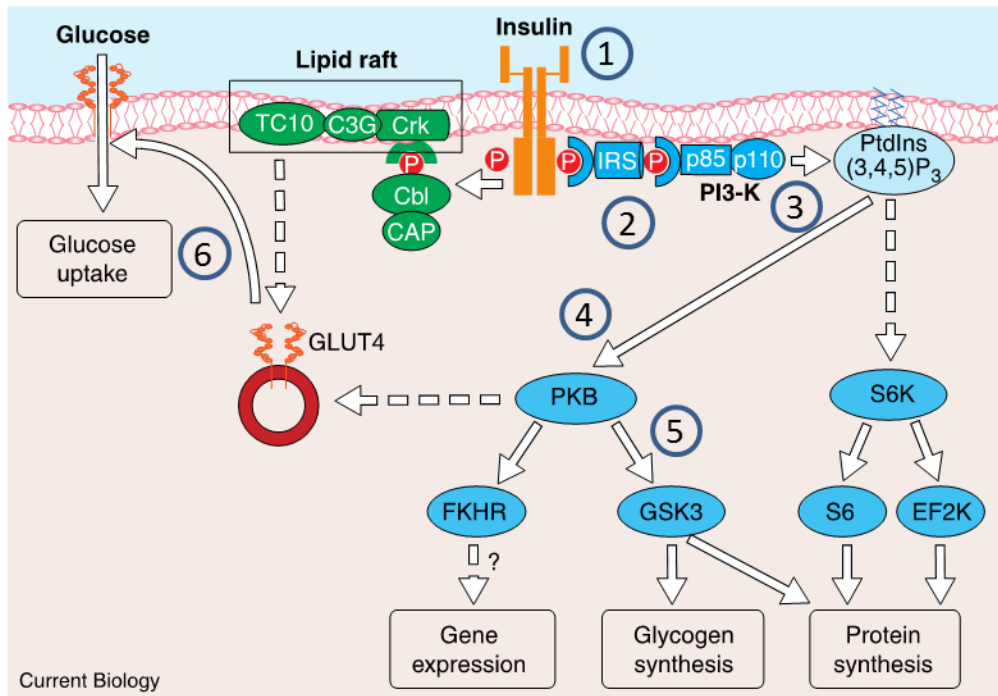


Figure 6: The insulin signaling pathway

(Lizcano JM, A.D., *The insulin signalling pathway*. *Curr Biol*, 2002. 12(7): p. R236-8)

1. The interaction of insulin with its receptor, leads to autophosphorylation at several tyrosine residues of the tyrosine kinase receptor.
2. This creates docking sites for Phosphoinositide 3-kinase (PI3K) leading to its recruitment at the plasma membrane.
3. PI3K then phosphorylates phosphatidylinositol (4,5) bisphosphate (PtdIns(4,5)P₂) to PtdIns(3,4,5)P₃.
4. A downstream effector of PtdIns(3,4,5)P₃ is protein kinase B (PKB), also known as Akt, which binds to PtdIns(3,4,5)P₃ via an amino terminus pleckstrin homology domain

leading to membrane recruitment. Complete activation of Akt requires phosphorylation at two sites – Thr 308 by PDK1 and Ser 473 by mTORC2.

5. Activated Akt then phosphorylates a range of substrates, which includes glycogen synthase kinase-3 (GSK3) leading to its inactivation. Glycogen synthase, which catalyzes the synthesis of glycogen, is the substrate for GSK3. When phosphorylated, glycogen synthase is inactivated. Thus, the inhibitory phosphorylation of GSK3 by Akt leads to the activation of glycogen synthase [54].
6. Glucose transporter 4 (GLUT4) is expressed in skeletal muscle and adipose tissue cells. In the absence of insulin, GLUT4 is excluded from the cell membrane and is sequestered in the cytoplasm. However, upon insulin stimulation, this transporter is translocated from the inside of the cell to the plasma membrane [55].

1.9 Growth hormone, insulin sensitivity and longevity

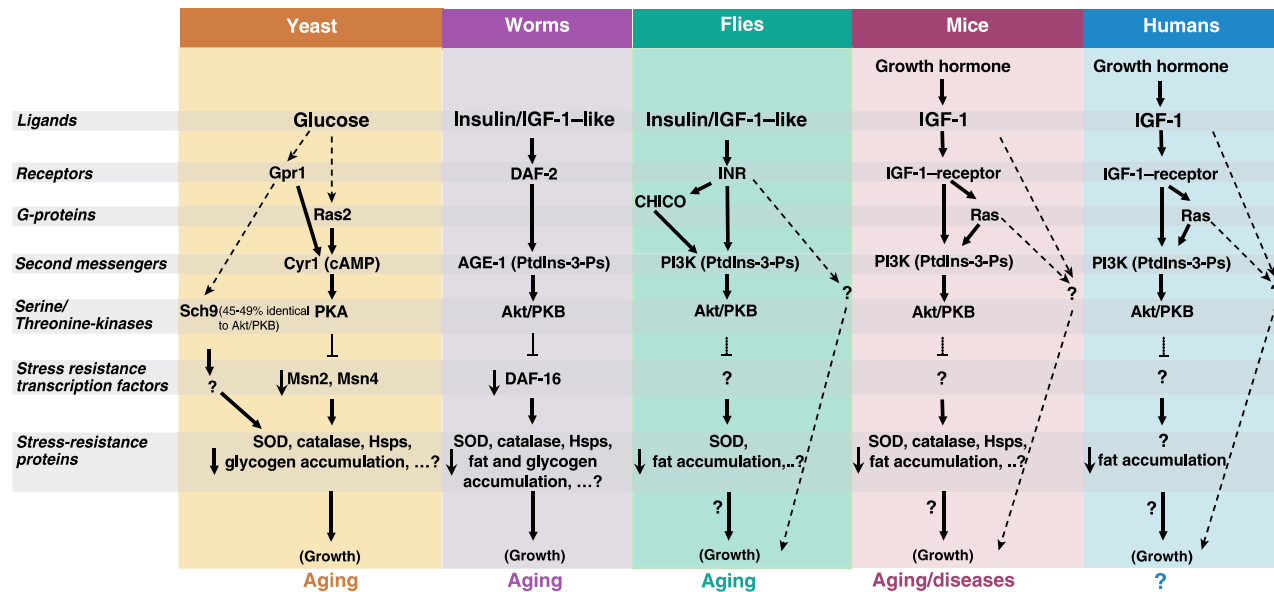


Figure 7: Mutations in growth-promoting pathways extend longevity and are conserved from yeast to mammals

(Longo VD, F.C., *Evolutionary medicine: from dwarf model systems to healthy centenarians?* Science, 2003. 299(5611): p. 1342-6)

In yeast, worms and flies, glucose and insulin/IGF-1 – like pathways lead to growth and aging of these organisms. These pathways lead to a decrease in the expression of antioxidant enzymes and heat shock proteins, lower accumulation of energy stores and an increase in mortality. However, mutations that suppress or perturb these pathways lead to an increase in longevity (figure 7) [56]. These ‘longevity pathways’ are conserved even in mammals. A study conducted by Holzenberger and colleagues showed that female IGF-1 receptor knockout mice (heterozygous) had increased lifespan and also exhibited higher resistance to oxidative stress, a factor that contributes to aging, suggesting that this receptor may regulate longevity [57].

As stated earlier, Ames dwarf mice have no production/secretion of GH leading to extremely low plasma levels of IGF-1. It was shown that the liver of *df/df* mice show increased expression of IR, IRS-1 and IRS-2 at the protein level as well as increased phosphorylation states of the insulin receptor substrate proteins, which could contribute to the enhanced insulin sensitivity of these mutants [58].

Growth hormone receptor knock out (GHRKO) mice, generated by targeted disruption of the GHR gene, have elevated levels of GH in circulation. However, due to the absence of functional receptors, these mice are characterized by GH-resistance. Thus, they have low circulating levels of IGF-1 [59]. The *df/df* and GHRKO mice exhibit increased longevity being very insulin sensitive and also have high plasma levels of adiponectin even with an increase in adiposity [3]. The liver of GHRKO mice exhibits higher expression of IR protein as well as increased tyrosine phosphorylation of the receptor, leading, at least in part, to the enhanced insulin sensitivity seen in these mice [60]. GHRKO mice are also protected from cancer [61]. It

is important to note that in both these mutant dwarf mice there is a disruption of GH signaling either due to the absence of GH (df/df mice) or due to the inability of secreted GH to signal via its receptor (GHRKO mice). Thus, suppression of the GH/IGF-1 (somatotropic) axis leads to extended longevity and insulin sensitivity in these mice.

The GHRKO mouse was generated as an animal model for Laron syndrome which affects humans. Subjects with this condition exhibit hereditary dwarfism due to a mutation in the GHR gene. Like the mouse model, these people exhibit a dwarf phenotype with central obesity, have low IGF-1 and high GH levels in circulation and due to non-functional GHR, are resistant to the actions of GH. The Laron dwarf humans are very insulin sensitive, showing no signs of diabetes and cancer [59, 62, 63]. In contrast, Transgenic mice overexpressing growth hormone have high circulating IGF-1 levels and increased adult body size. These giant animals are characterized by a decreased lifespan and insulin resistance [64]. Humans with a pathological excess of growth hormone (acromegaly) are also insulin resistant [34, 65] and usually do not live long. Moreover, administering GH to Ames dwarf mice early in life leads to a decrease in their longevity (figure 8) [66] and also to reduced insulin sensitivity [67].

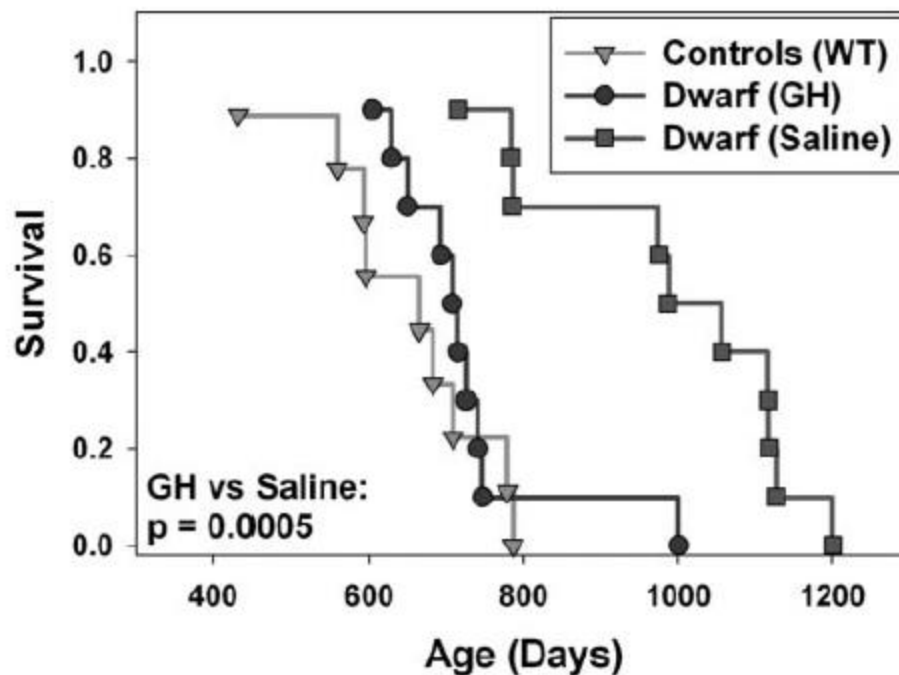


Figure 8: Decreased longevity of df/df mice upon early-life GH treatment
(Panici JA, H.J., Miller RA, Bartke A, Spong A, Masternak MM, Early life growth hormone treatment shortens longevity and decreases cellular stress resistance in long-lived mutant mice. FASEB J, 2010. 24(12): p. 5073-9)

As mentioned above, df/df and GHRKO mice live significantly longer than their wild-type controls. Calorie restriction further extends the lifespan of df/df mice. In other words, df/df mice live longer than N mice, but by restricting calorie intake they live even longer. This extension of longevity is reflected in insulin sensitivity; df/df mice are already very insulin sensitive compared to N mice, but have a further increase in insulin sensitivity when on CR [68]. However, long-living GHRKO mice do not benefit from CR in terms of longevity, and when subjected to CR, they do not show any further increase in insulin sensitivity. Thus, there is a probable link between longevity and insulin sensitivity [68].

CHAPTER 2: MATERIALS AND METHODS

2.1 Experimental animals

Ames dwarf and control mice used in this study were developed by crossing normal heterozygous ($df^{+/-}$) female with homozygous Ames dwarf male mice, thus 50% of the F1 population were mutant. The *prop1* mutation was maintained on a heterozygous background. All mice were maintained in temperature controlled conditions (20-20⁰C) under 12h light/12h dark cycles. They had free access to drinking water and standard laboratory chow diet. Ames dwarf mice were weaned at 41 days while N mice were weaned at the usual 21 days.

2.2 Visceral fat removal (VFR)

Only male mice were used in this study. Ames dwarf and N mice, 3-6 months old, were categorized into two groups (n = 9 – 10) – visceral fat removal (VFR) or sham-operated. Surgical procedures were performed with mice under ketamine/xylazine anesthesia. Mice were shaved and prepped as usual. Ibuprofen was supplied via water 2 days before the surgery and 3 days after. Animals in the VFR group underwent surgical excision of the major VF depots. Epididymal fat was removed via a blunt dissection through a vertical midline incision, ensuring no damage was done to any blood vessels or the epididymis. Perirenal fat was removed by two flank incisions. As much fat as possible was collected without disrupting blood flow or damaging any organs. The excised fat was weighed and snap-frozen in liquid nitrogen and stored at -80⁰C until further analysis. For mice in the sham-operated group, incisions were made at the

same positions as on VFR animals, and VF was mobilized, but not removed. Animals were closely monitored for recovery post-surgery.

2.3 Fat adiponectin and serum IL-6 levels

Animals used for analyzing the levels of adiponectin in different fat pads and IL-6 in serum were about a year old. After an overnight fast, df/df (n=10) and N (n=10) mice were anesthetized with isoflurane. Blood was collected by cardiac puncture. Mice were sacrificed by cervical dislocation. Different fat pads (EF, PR and SQ) were collected and snap frozen in liquid nitrogen. Proteins were extracted from these fat depots before storing the tissues at -80⁰C.

2.4 Analysis of glucose tolerance and whole-body insulin sensitivity

Approximately a month after surgery, mice were subjected to a glucose tolerance test (GTT) to determine their ability to clear blood glucose. After overnight fasting, body weights were determined and the tail was snipped to collect blood samples. A baseline blood glucose measurement (0 min) was made using a standard glucometer. The mice were then injected intraperitoneally with glucose (2g glucose per kg body weight) and blood glucose levels were measured at defined time points (15 min, 30 min, 45 min, 60 min and 120 min). A week after GTT, an insulin tolerance test (ITT) was administered to these animals to determine their sensitivity to injected insulin at the whole-body level. For this, after body weights were determined and baseline blood glucose (0 min) measured, nonfasted mice were administered insulin (1 IU insulin/kg body weight) via an intraperitoneal injection. Blood glucose levels were checked at specific time points (15 min, 30 min, 45 min and 60 min).

2.5 Insulin stimulation and tissue collection

Three months after surgery, mice were fasted overnight and then anesthetized with ketamine/xylazine. Blood was collected by cardiac puncture. In each group of mice, animals (approximately 50%) were injected with either a high dose of insulin (10 IU insulin/kg body weight) or saline (control) via the inferior vena cava to stimulate insulin signaling in target organs. Exactly 2 minutes after injection, mice were sacrificed by cervical dislocation, and tissues were collected and snap-frozen in liquid nitrogen and stored at -80°C till further analysis. At the time of tissue collection, no visible regrowth of fat was seen in the animals that had undergone VFR

2.6 RNA extraction from frozen tissue

RNA was extracted from skeletal muscle and adipose tissues using miRNeasy mini kit (Qiagen). Approximately 50 mg tissue was cut on dry ice. 300ul Qiazol reagent was added to each tube of frozen tissue. The samples were homogenized with zirconium oxide beads (1.0 mm for skeletal muscle and 0.5 mm for adipose tissue) using the bullet blender ® (Next advance) homogenizer (Skeletal muscle: speed 10, 3 minutes; adipose tissue: speed 8, 3minutes). Each tube was centrifuged for a few seconds and then 400ul of Qiazol was added and mixed by gently inverting the tubes, which were then allowed to incubate at room temperature for 5 min. RNA extraction from adipose tissue involved the additional step of centrifuging the samples at 12000 x g for 10 min at 4°C , after which the upper lipid layer was excluded and only the infranatant was transferred to a new tube. 140ul chloroform was then added and mixed by inverting the tubes

followed by incubation at room temperature for 3 minutes. Phase separation was achieved by centrifuging the tubes at 12,000 x g for 15 minutes at 4⁰C. The aqueous phase was transferred to a new tube followed by ethanol-precipitation of the RNA. Each sample was then passed through the RNeasy Mini spin column which bound RNA. The columns were then washed with buffers provided in the kit. DNase digestion was performed on-column. Pure RNA was eluted using 50ul and 30ul nuclease-free water (provided in the kit) for skeletal muscle and adipose tissue samples respectively. The concentration and purity of the eluted RNA samples were determined using the Take3 plate and the Epoch plate reader (BioTek). RNA samples with $A_{260}/A_{280} < 1.9$ were re-extracted. Extracted RNA samples were stored at -80C until further use.

2.7 cDNA synthesis

Complementary DNA was synthesized from extracted RNA samples using iScript™ cDNA Synthesis Kit (Bio-Rad) (Skeletal muscle and epididymal fat) or EasyScript Plus™ cDNA Synthesis Kit (Applied Biological Materials) (Subcutaneous fat). 1 ug of RNA was used per reaction.

Table 1: cDNA synthesis using iScript™ cDNA Synthesis Kit (Bio-Rad)

Components	Volume per reaction
5x iScript reaction mix	4 ul
iScript reverse transcriptase	1 ul
Nuclease-free water	Volume adjusted to 20ul
RNA template	Scaled to 1ug
Total	20 ul

The following protocol was followed using the MJ Mini thermal cycler (Bio-Rad)

Table 2: Run protocol for iScript™ cDNA Synthesis Kit (Bio-Rad)

Temperature	Duration
25 ⁰ C	5 min
42 ⁰ C	30 min
85 ⁰ C	5 min
4C	Forever

Table 3: cDNA synthesis using EasyScript Plus™ cDNA synthesis kit (Applied Biological Materials)

Component	Volume
Total RNA	Scaled to 1ug
Random primer (10um)	1ul
dNTP (10mM)	1ul
5X RT buffer	4ul
RNaseOFF ribonuclease inhibitor (40 U/ul)	0.5ul
EasyScript Plus™ Rtase (200 U/ul)	1ul
RNase-free H ₂ O	Volume adjusted to 20ul

Table 4: Run protocol for cDNA synthesis with EasyScript Plus™ cDNA synthesis kit (Applied Biological Materials)

Temperature	Duration
25 ⁰ C	10 min
50 ⁰ C	50 min
85 ⁰ C	5 min
4 ⁰ C	Forever

2.8 Quantitative real-time polymerase chain reaction (qPCR)

Relative gene expression was analyzed by qPCR using Fast SYBR® Green Master Mix (Applied Biosystems) on 7900 HT fast real-time PCR system (Applied Biosystems). Each run had the following steps:

- 1) Enzyme activation at 95⁰C for 20 sec
- 2) Denaturation at 95⁰C for 1 sec
- 3) Annealing/extension at 62⁰C for 20sec

Table 5: qPCR reaction mix components

Component	Volume per reaction
Fast SYBR® Green Master Mix	5 ul
Forward primer (10uM)	0.2 ul
Reverse primer (10um)	0.2 ul
cDNA	2.0 ul
Nuclease-free water	12.6 ul
Total	20 ul

Based on the Ct values of the housekeeping gene (b-2-microglobulin), the cDNA was diluted with nuclease-free water. Each sample was run in two replicates.

Table 6: Primer sequences for qPCR

Gene	Primer sequences (Forward and reverse)
B2M	F: 5'-AAGTATACTCACGCCACCCA-3' R: 5'-CAG CGC TAT GTA TCA GTC TC-3'
IR	F: 5'-GTTCTTTCCTGCGTGCATTTCCCA-3' R: 5'-ATCAGGGTGGCCAGTGTGTCTTTA-3'
IRS-1	F: 5'- AGCCAAAAGCCCAGGAGAATA-3' R: 5'-TTCCGAGCCAGTCTCTTCTCTA-3'
IRS-2	F: 5'-AGTAAACGGAGGTGGCTACA-3' R: 5'-AAGCTGAGAAGTCAAGGT-3'
PI3K	F: 5'-TAGCTGCATTGGAGCTCCTT-3' R: 5'-TACGAACTGTGGGAGCAGAT-3'
Akt2	F: 5-GAGGACCTTCCATGTAGACT-3' R: 5'-CTCAGATGTGGAAGAGTGAC-3'
GLUT4	F: 5'-ATTGGCATTCTGGTTGCCCA-3' R: 5'-GGTTCCGGATGATGTAGAGGTA-3'
PPAR γ	F: 5'-GTCAGTACTGTCGGTTTCAG-3'

	R: 5'-CAGATCAGCAGACTCTGGGT-3'
Pgc1 α	F: 5'-TACGCAGGTCGAACGAAACT-3' R: 5'-TGCTCTTGGTGGGAAGCA-3'
TNF α	F: 5'-TAGCAAACCACCAAGTGGAG-3' R: 5'-AACCTGGGAGTAGACAAGGT-3'
IGF-1	F: 5'-CTGAGCTGGTGGATGCTCTT-3' R: 5'-CACTCATCCACACCTGT-3'

2.9 Protein extraction from frozen tissue

Total proteins were extracted from skeletal muscle and adipose tissues using T-PER Tissue Protein Extraction Reagent (with protease and phosphatase inhibitor) (Thermo Scientific). Samples were homogenized in the extraction buffer using the Bullet blender homogenizer as mentioned earlier. After centrifugation at 12,000 x g for 15 minutes at 4⁰C, the layer below the fat was collected into a new tube and centrifuged again. The relatively fat-free protein extract was then quantified using the BCA assay (Thermo Scientific). For the quantification assay, protein samples were diluted 1:10 with T-per.

2.10 Western blotting

Criterion™ TGX™ Precast Gels (10%) and Criterion™ Cell running tank (Bio-Rad) were used for SDS-PAGE. A total amount of 60ug protein was loaded in each well of the gel. Protein samples for Western blotting were prepared in Laemmli sample buffer (final concentration of 1X) (Bio-Rad) and boiled for 5 min in a dry bath (MidSci). Samples were centrifuged for a few seconds and then loaded onto the gel. Odyssey Protein Molecular Weight Marker (Li-cor) was used. Tris/Glycine/SDS (TGS) Electrophoresis Buffer (Bio-Rad) was used as the running buffer at a final concentration of 1X. SDS-PAGE was carried out at 100V for ~2h. After the run, the gel sandwich was assembled: sponge – filter paper – gel – membrane (PVDF) – filter paper – sponge. Transfer was carried out at 80 V for 45 min in the Criterion™ Blotter (Bio-Rad) using chilled Tris/Glycine (TG) buffer (Bio-Rad) with 20% methanol as the transfer buffer (final concentration 1X). After transfer, the membrane was rinsed with PBS for 3 min and then blocked with 5% milk (in PBS) for 1 hour at room temperature with gentle agitation. The

membrane was then rinsed with PBS-T for 30 min (5 min washes), and incubated with 1⁰ antibody at 4⁰C overnight with gentle shaking. (1⁰ antibody buffer = Odyssey blocking buffer + PBS-T (1:1)). After rinsing the membrane for 30 min (5 min washes), it was incubated with 2⁰ antibody for 1 hour at room temperature (2⁰ antibody buffer = Odyssey blocking buffer + PBS-T (1:1) + 0.02% SDS). The membrane was then washed for 30 min (5 min washes) and was imaged using the Odyssey imaging system (Li-cor) with Image studio (2.1) software. All primary antibodies (host: rabbit) were purchased from Cell Signaling Technology: α - Akt (# 9272), α -Phospho-Akt (Ser473) (# 4060) and α -Phospho-Akt (Thr308) (# 4056). Anti-rabbit secondary antibody was purchased from Li-cor (IRDye® 800CW Goat (polyclonal) Anti-Rabbit IgG). The equal intensity of non-specific bands, as revealed upon staining the membrane with the ‘reversible protein stain’ (Thermo Scientific), was used as a loading control.

2.11 Enzyme-linked immunosorbent assay (ELISA) for adiponectin (plasma)

Mouse adiponectin ELISA kit (Invitrogen) was used to analyze the levels of adiponectin in plasma. Briefly, the plasma samples were diluted with diluent provided in the kit (dilution factor = 20,000). 100ul of standards, samples and QC samples were loaded on to the antibody-coated plate and incubated at 37⁰C for 1 hour. The plate was then washed 3 times with 250ul wash solution (1X) using the ELx50 plate washer (BioTek), and incubated at 37⁰C for 1 hour with secondary antibody. After washing 3 times, the detector (1X) was added to the plate which was then incubated at 37⁰C for another hour. The plate was washed 5 times. After adding 100ul substrate solution, the plate was incubated in the dark at room temperature for 20 minutes. The

reaction was stopped by adding 100ul of the stop solution and the plate was read at 450 nm using the Epoch plate reader (BioTek).

2.12 Enzyme-linked immunosorbent assay (ELISA) for adiponectin (adipose tissue)

Proteins were extracted and quantified from the different fat pads (epididymal, perirenal and subcutaneous) of df/df and N mice as mentioned above. Extracted proteins were adjusted to a concentration of 0.5ug/ul in a total volume of 60ul in the same extraction buffer (T-PER) and then diluted to a concentration of 0.0025 ug/ul using the diluent buffer (1X) from the kit to a final volume of 800ul. The protocol as mentioned above was then followed.

2.13 Enzyme-linked immunosorbent assay (ELISA) for insulin (plasma)

Ultra sensitive mouse insulin ELISA kit (Crystal Chem) was used for the analysis of insulin in plasma. 95ul of sample diluent, provided in the kit, and 5ul plasma samples were added to the antibody coated microplate and incubated at 4⁰C for 2 hours. The wells were then washed 5 times with 300ul of wash buffer and then incubated with 100ul of anti-insulin enzyme conjugate at room temperature for 30 min. The plate was then washed 7 times with 300ul of wash buffer followed by incubation, in the dark, with 100ul of enzyme substrate solution at room temperature for 40 min. After adding 100ul of stop solution to each well, the absorbance was measured at 450nm and 630nm using the Epoch plate reader (BioTek).

2.14 Bio-Plex Pro™ Assay for IL-6 levels in serum

Interleukin-6 levels in serum of df/df and N mice were detected using the Bio-plex assay (Bio-Rad). In brief, the Bio-plex 200 instrument was warmed up, calibrated and validated. 50ul

of magnetic beads were added to the assay plate and washed 2 times with 100ul wash buffer using a Handheld Magnetic Washer (Bio-Rad). 50ul samples and standards were added to the plate which was protected from light and incubated at room temperature for 30 min on a shaker at 300 rpm. The plate was then washed 3 times with wash buffer, and 25ul of detection antibody was added, followed by incubation as before. After another wash cycle (3 times), 50ul of streptavidin-PE was added to the plate and incubated at room temperature on a shaker at 300 rpm (protected from light) for 10 min. After a final wash step (3 times) the beads were resuspended in 125ul assay buffer by agitating on a shaker at 1100 rpm for 30 sec. The plate was then read using the Bio-plex 200 system and Bio-plex manager 6.0 software.

CHAPTER 3 RESULTS

3.1 Body weight and visceral fat content

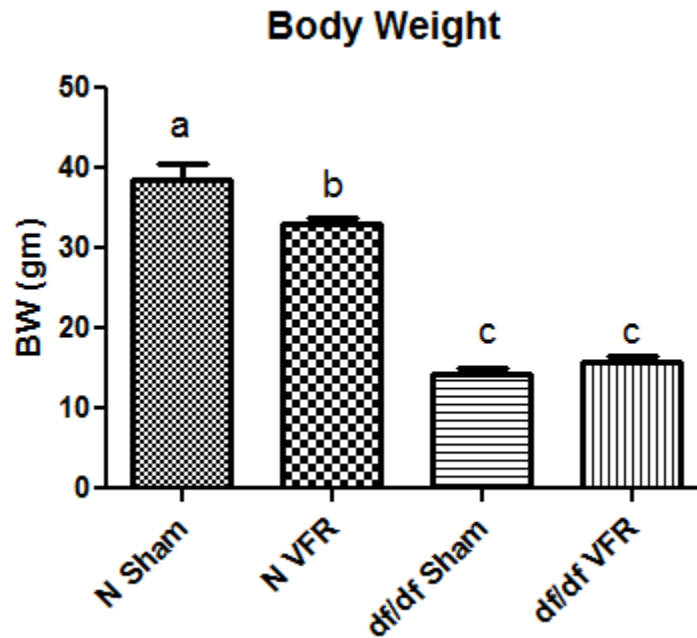


Figure 9: Effect of VFR on body weight of df/df and N mice

Ames dwarf mutants were one-third the size of N mice ($p < 0.0001$). Surgical removal of visceral fat led to a significant reduction in the (fasted) body weight of N mice only ($p = 0.0094$)

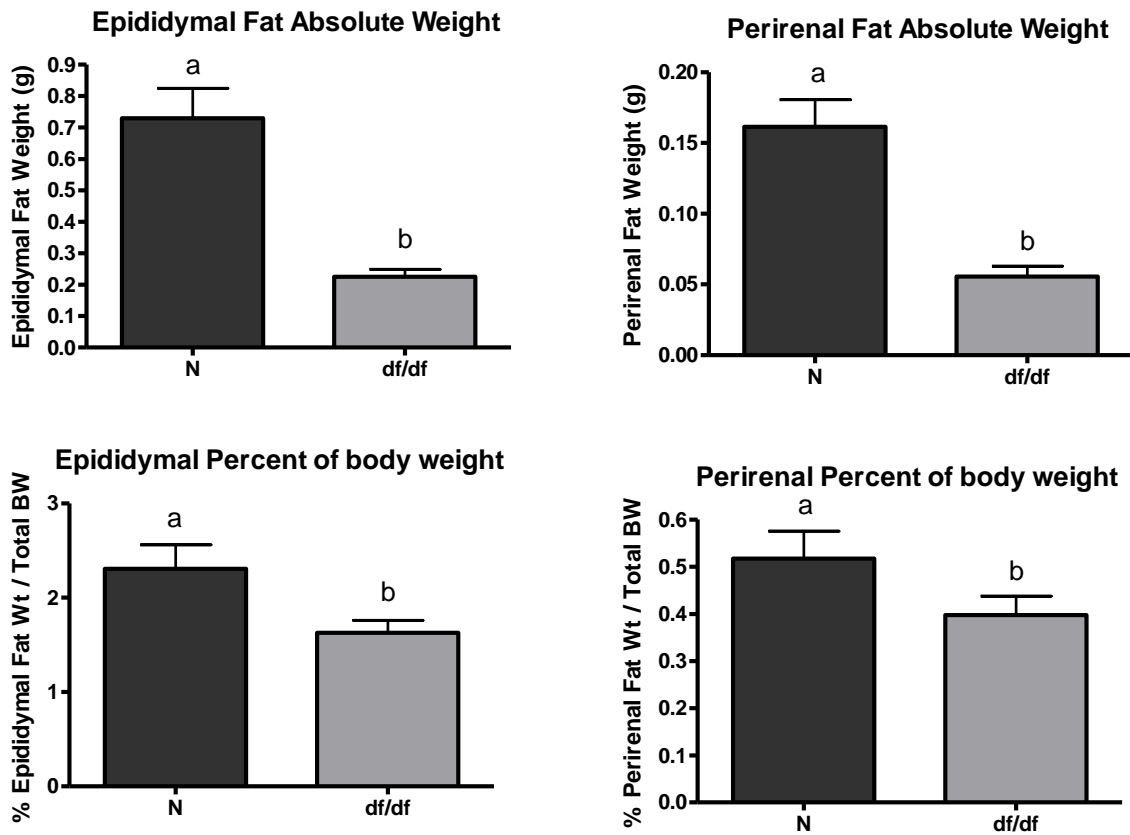


Figure 10: Visceral fat content (absolute and percentage of body weight) of N and df/df mice

The weight of the fat pads removed from mice in the VFR group was measured at the time of surgery. Ames dwarf mice had a decreased amount of absolute visceral fat ($p < 0.0001$). The relative amount of epididymal and perirenal fat (percentage of body weight) was also lower in df/df compared to N mice ($p = 0.0067$ and $p = 0.0439$ respectively).

3.2 Whole-body insulin sensitivity

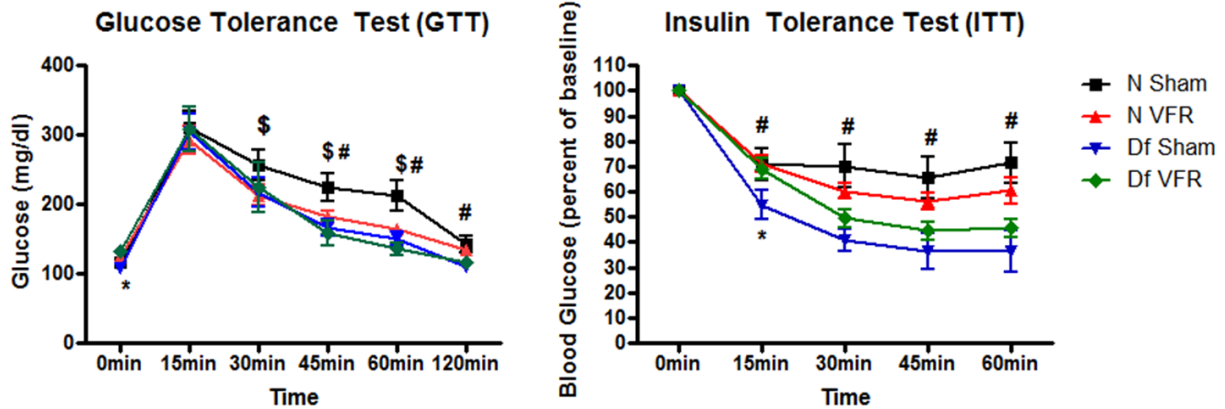


Figure 11: Glucose tolerance test (GTT) and insulin tolerance test (ITT)

(\$, * and # indicates a significant difference ($P < 0.05$) between the measured parameters in N Sham and N VFR, df/df sham and df/df VFR and N Sham and df/df sham mice respectively)

As indicated by the glucose tolerance test, surgical removal of visceral fat improved glucose tolerance only in N mice. There was a significant difference in blood glucose between N mice in the sham-operated and VFR groups at the following time points: 30 min ($p = 0.0436$), 45 min ($p = 0.0274$) and 60 min ($p = 0.0249$). The difference in blood glucose between N sham and df/df sham mice was significant only at 45 min ($p = 0.0079$), 60 min ($p = 0.0104$) and 120 min ($p = 0.0100$) time points. At time 0 min, mice in the df/df sham group had a significantly lower blood glucose level than mice in the df/df VFR group ($p = 0.0028$).

The insulin tolerance test revealed that mice in the df/df sham group were very insulin sensitive compared to N sham mice and reached statistical significance at the different time

points when blood glucose levels were measured: 15 min ($p = 0.0381$), 30 min ($p = 0.0038$), 45 min ($p = 0.0090$) and 60 min ($p = 0.0034$). The effect of VFR on insulin sensitivity in *df/df* mice was statistically significant only at the 15 min time point ($p = 0.0297$). There was significant genotype/intervention interaction for GTT and ITT as determined by repeated measures ANOVA test ($p = 0.0310$ and $p = 0.0006$ respectively).

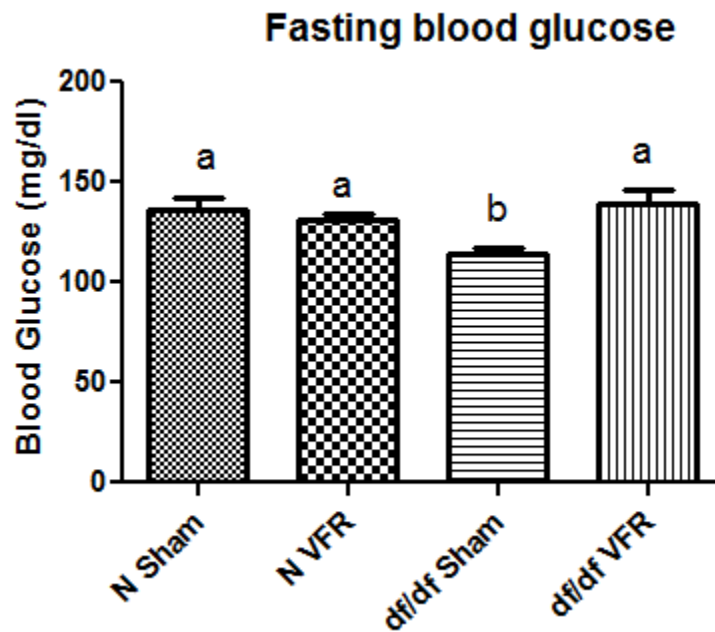


Figure 12: Effect of VFR on fasting blood glucose levels

Ames dwarf mice had low blood glucose levels compared to N mice ($p = 0.0014$). Surgically removing visceral fat led to an increase in the blood glucose level of *df/df* mice ($p = 0.0020$) with no change in the controls.

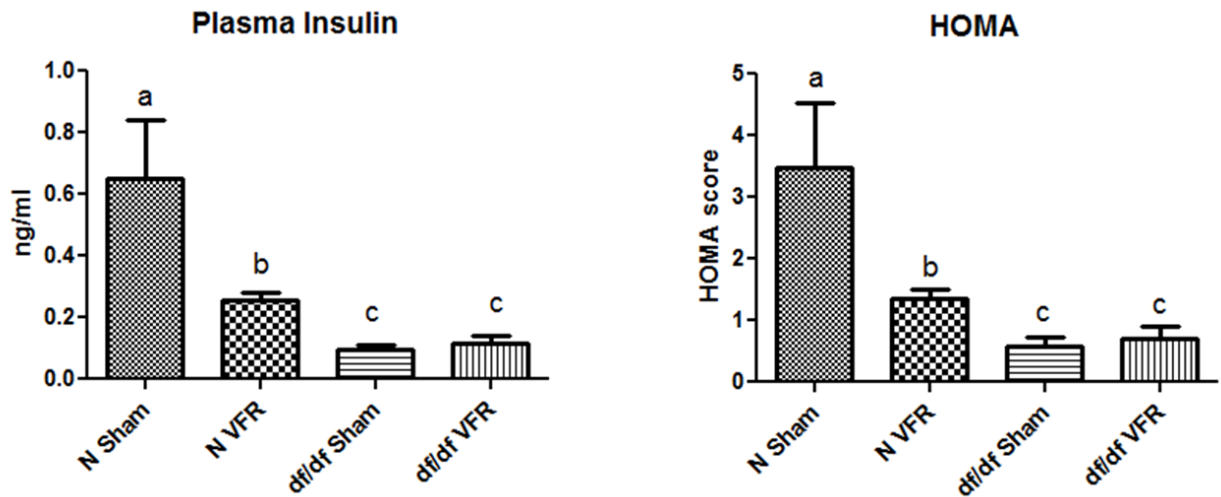
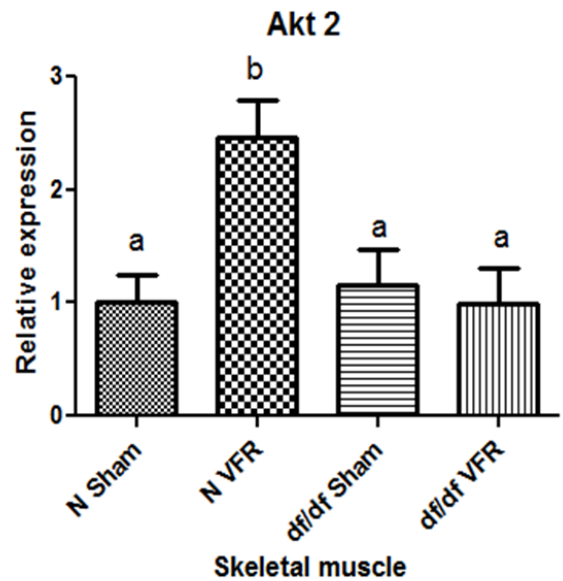
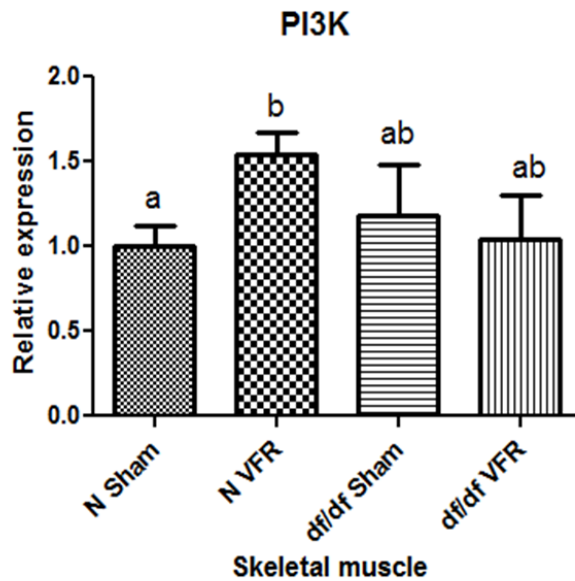
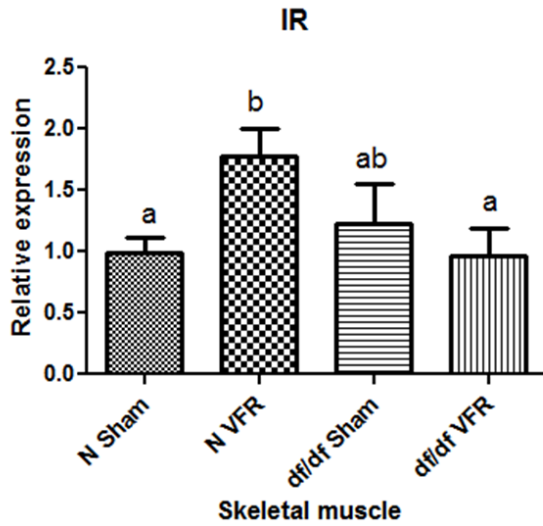


Figure 13: Plasma insulin levels and HOMA score

Ames dwarf mice had significantly low levels of insulin in circulation, relative to N mice ($p = 0.0125$), as measured by ELISA. Visceral fat removal decreased insulin levels in plasma of N mice only ($p = 0.0233$) with no change in df/df mice. As seen by the homeostatic model assessment (HOMA) score, Ames dwarf mice were very insulin sensitive compared to the wild-type littermates ($p = 0.0153$). Also, in parallel with decreased plasma insulin levels, surgical removal of visceral fat depots significantly improved insulin sensitivity in the control mice ($p = 0.0306$) with no change in the mutant dwarfs.

3.3 Effect of VFR on expression of insulin signaling genes in skeletal muscle



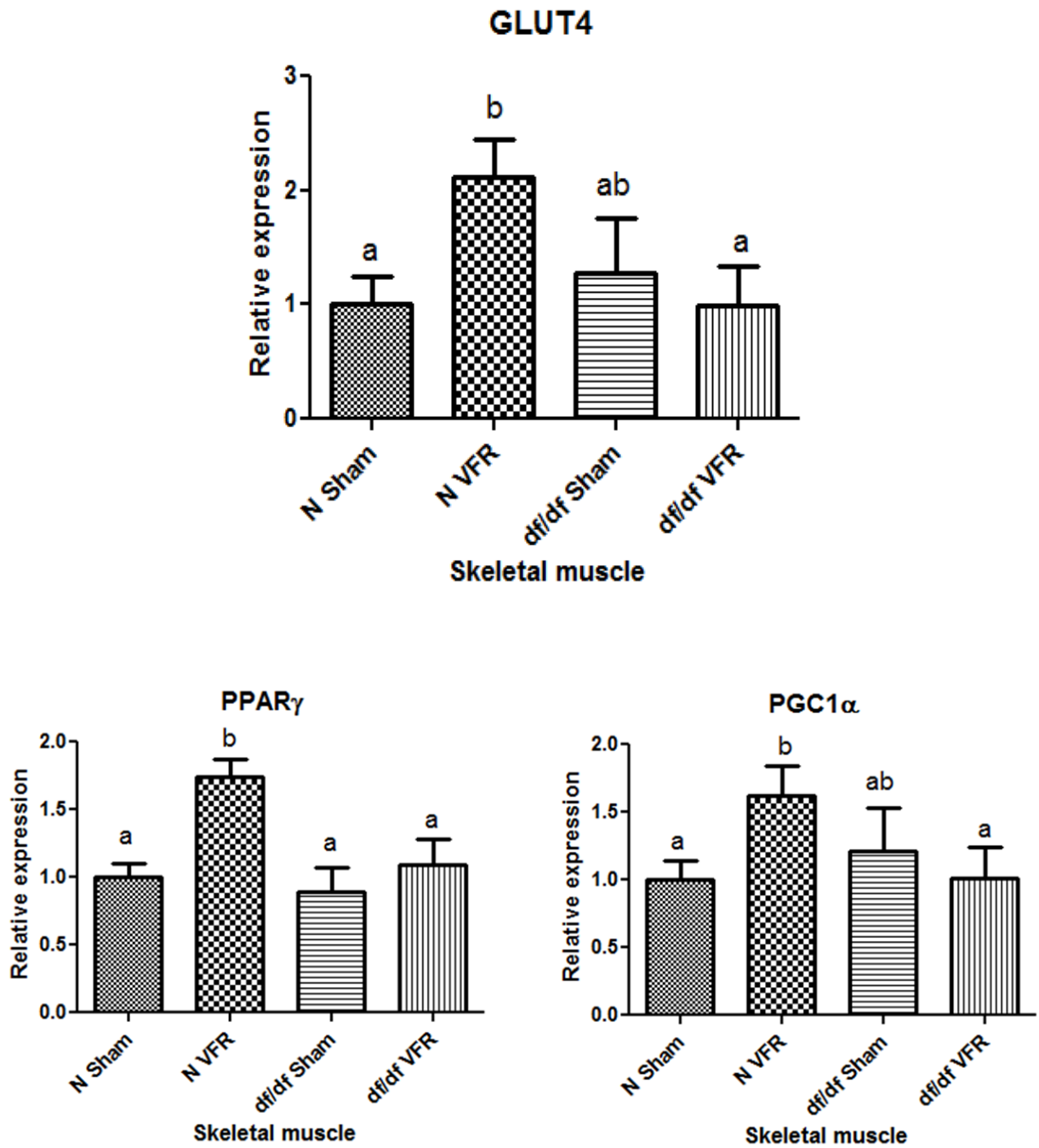


Figure 14: Differential gene expression upon VFR in skeletal muscle of N and df/df mice

Surgically removing visceral fat resulted in an upregulation of several genes involved in the insulin signaling pathway, as determined by qPCR, in skeletal muscle of N mice only with no

significant changes in df/df mice. The expression of insulin receptor (IR), insulin receptor substrate-2 (IRS-2), phosphoinositide 3-kinase (PI3K), Akt2, GLUT4, Peroxisome proliferator-activated receptor gamma (PPAR γ) and Peroxisome proliferator-activated receptor gamma coactivator 1-alpha (PGC1 α) was increased at the mRNA level in skeletal muscle of normal mice upon VFR compared to the sham-operated group ($p = 0.0054$, $p = 0.0046$, $p = 0.0032$, $p = 0.0014$, $p = 0.0085$, $p = 0.0002$ and $p = 0.0187$ respectively).

3.4 Effect of VFR on the phosphorylation state of Akt in skeletal muscle

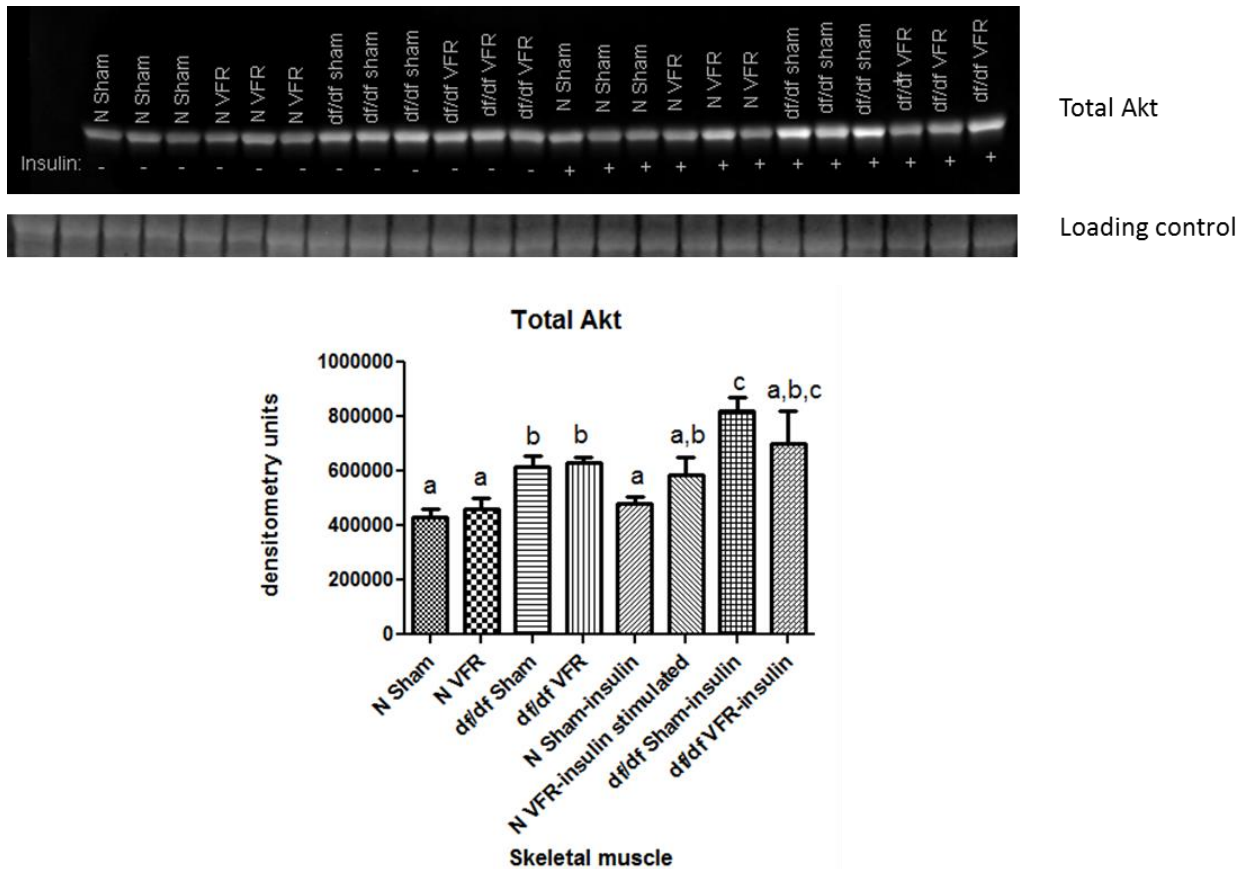
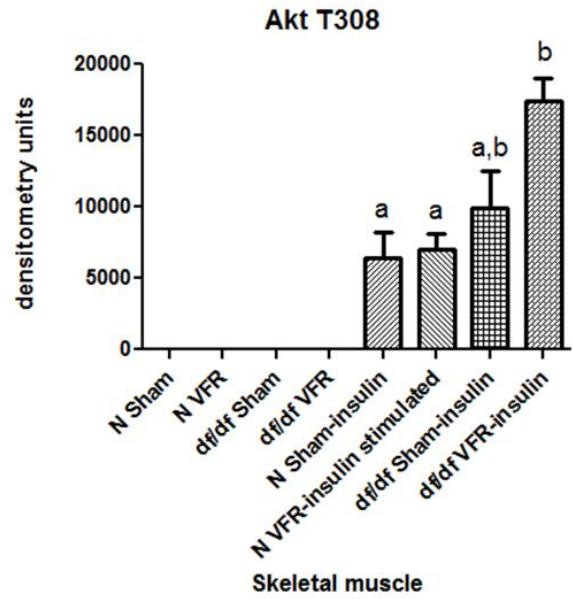
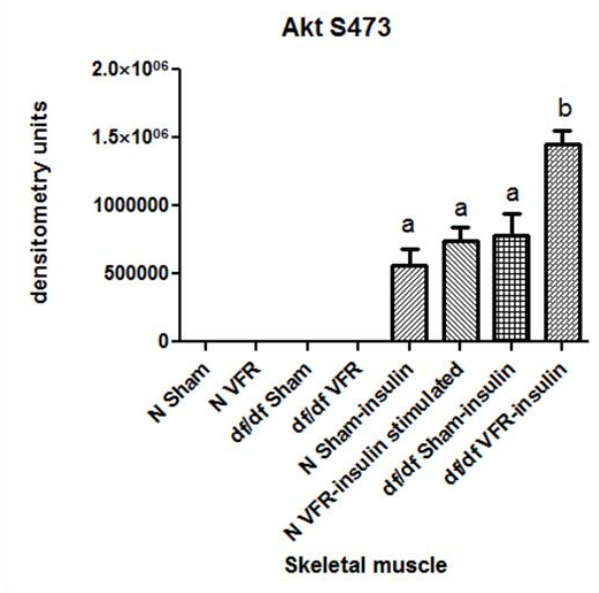
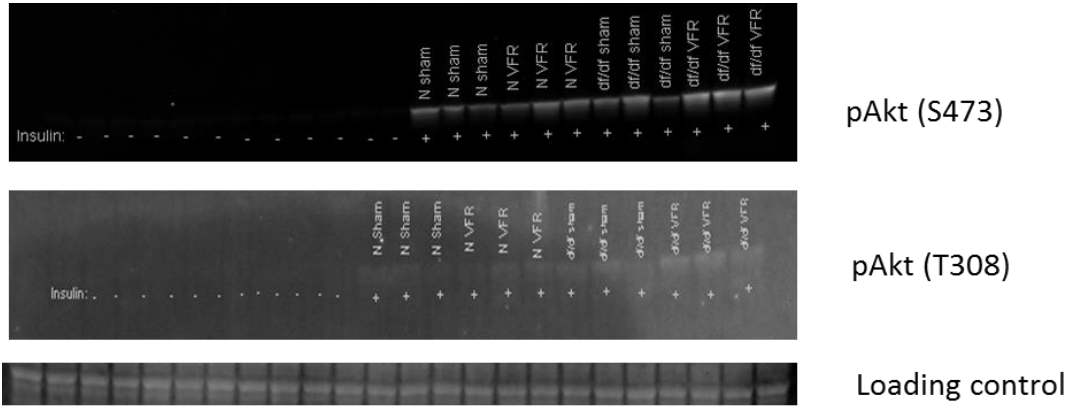


Figure 15: Expression of total Akt protein in skeletal muscle

Ames dwarf mice exhibited higher expression of total Akt protein in the skeletal muscle compared to N mice in insulin-stimulated and unstimulated states.



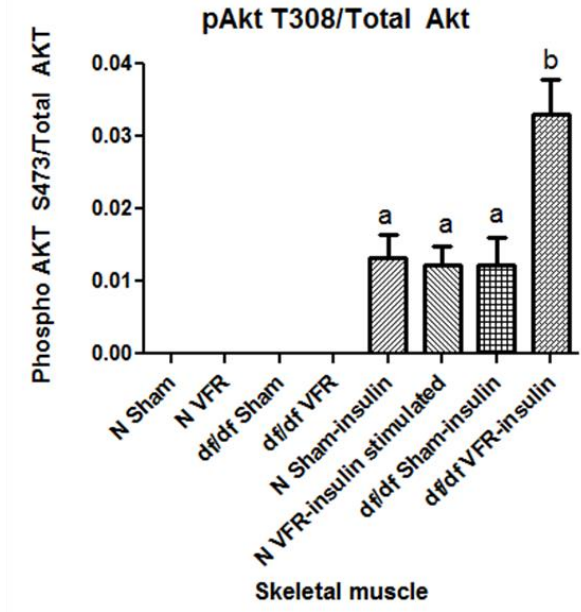
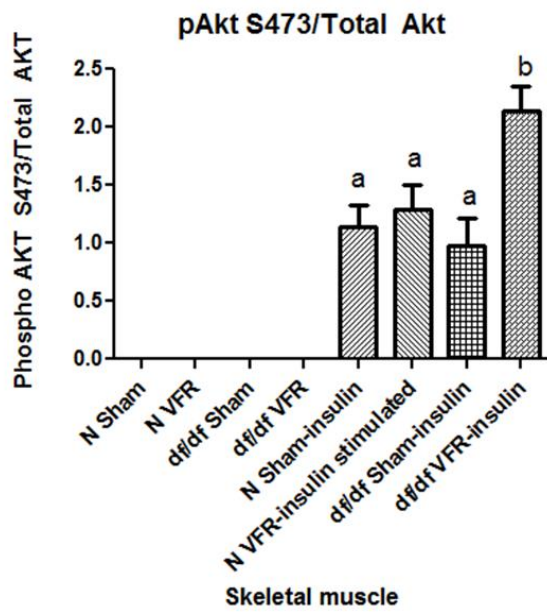
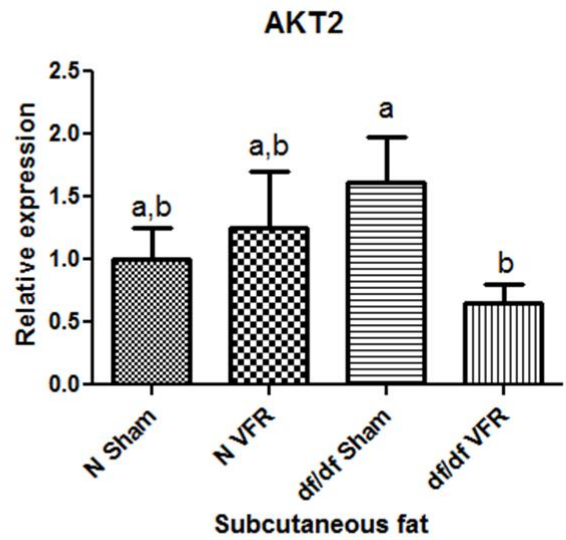
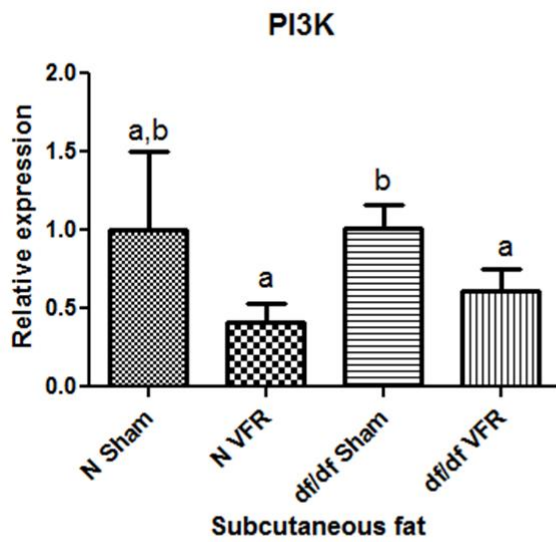
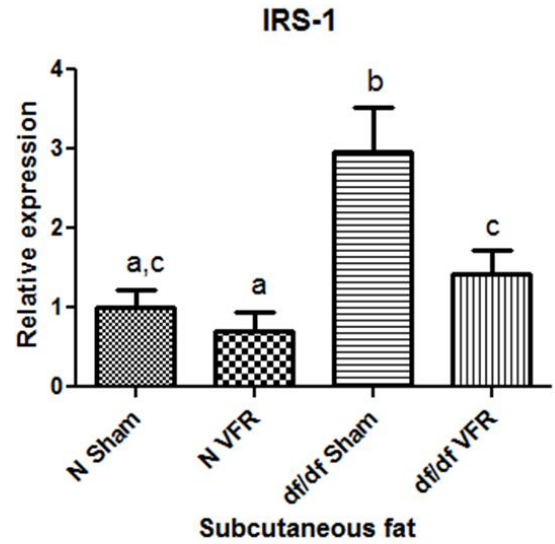
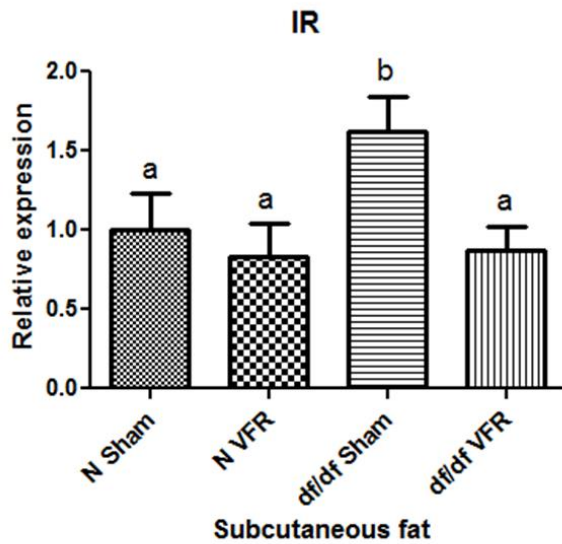


Figure 16: Effect of VFR on phosphorylation levels of Akt in skeletal muscle

No phosphorylation signal was seen in the groups treated with saline. The highest level of phosphorylation of Akt at S473 and T308 was observed in df/df mice that had undergone surgical removal of visceral fat depots. The ratio of pAkt to Akt also showed the greatest level of Akt activation (phosphorylation) in the df/df VFR group.

3.5 Effect of VFR on expression of insulin signaling genes in subcutaneous fat



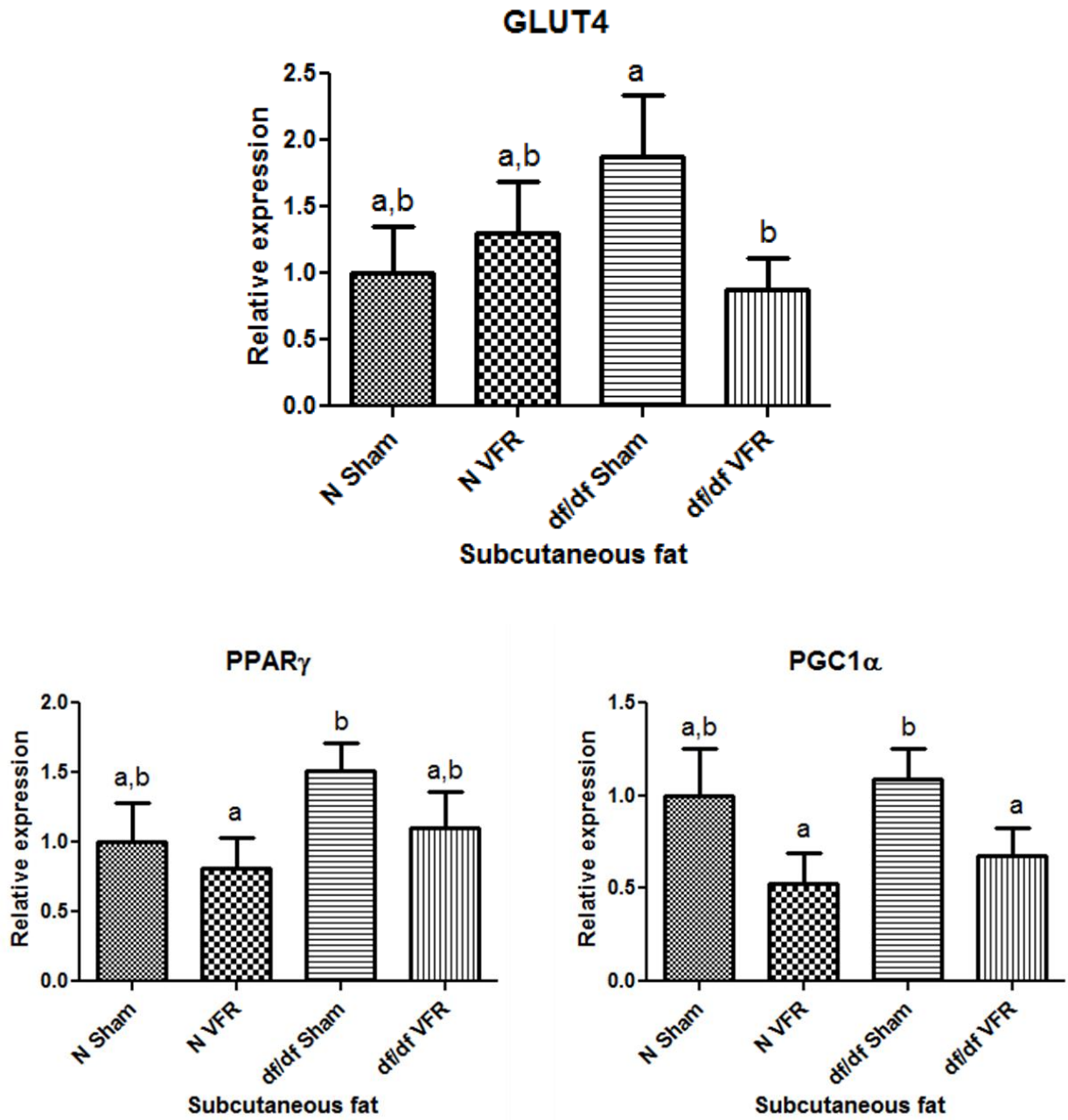


Figure 17: Effect of VFR on gene expression in subcutaneous fat

VFR lead to a decrease in the expression of the following genes in the subcutaneous fat of df/df mice only: IR, IRS-1, PI3K, Akt2, GLUT4 and PGC1a ($p = 0.0057$, $p = 0.0115$, $p = 0.0362$, $p = 0.0098$, $p = 0.0326$ and $p = 0.0428$ respectively). The expression of IR and IRS-1 transcripts was higher in the df/df sham-operated group compared to the control mice in the sham-operated group ($p = 0.0336$, $p = 0.0019$ respectively).

3.6 Local expression of IGF-1 in different tissues of the Ames dwarf mouse

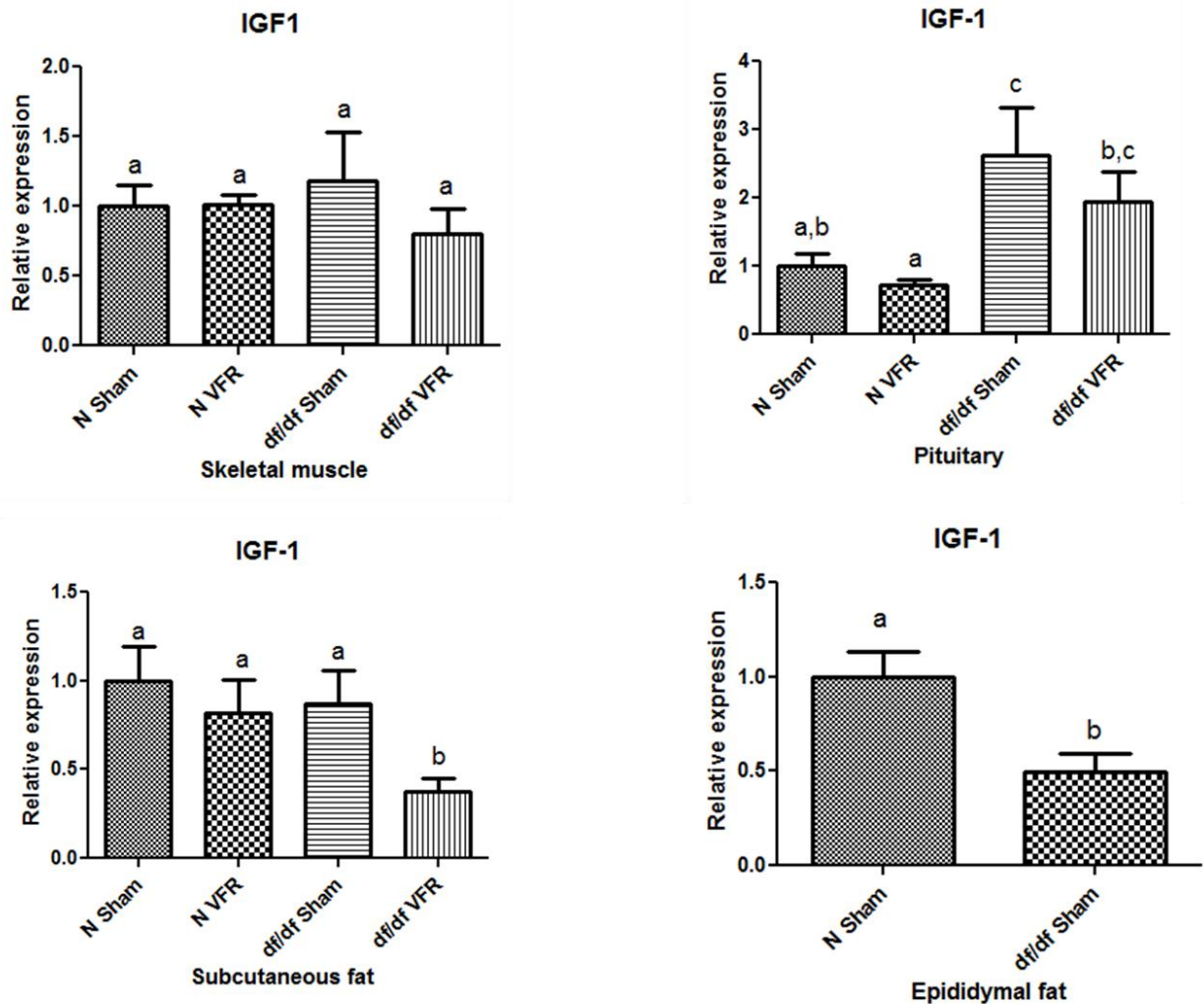


Figure 18: Local expression of IGF-1 in different tissues of df/df mice

As indicated by qPCR analysis, IGF-1 was expressed at the mRNA level in skeletal muscle, pituitary and adipose tissue (SQ and EF) of df/df mice. The gene expression of IGF-1 was significantly higher in the pituitary ($p = 0.046$) and lower in the EF ($p = 0.0033$) of df/df

mice compared to N mice in the sham-operated group. VFR caused a significant decrease in the expression of IGF-1 in SQ fat of df/df mice ($p = 0.0087$).

3.7 Differential gene expression levels in epididymal fat could contribute to enhanced insulin sensitivity in Ames dwarf mice

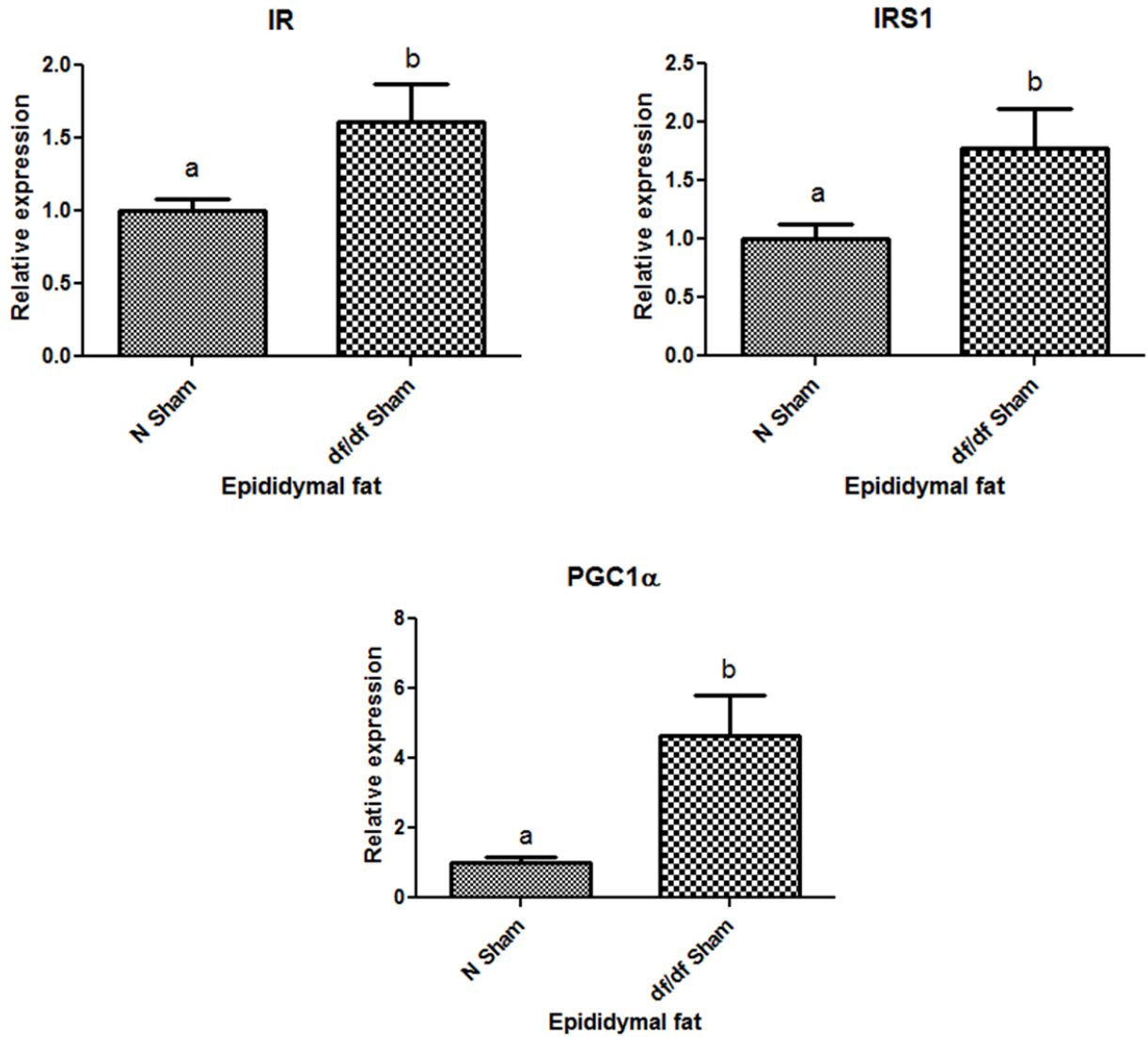


Figure 19: Increased expression of genes promoting insulin sensitivity in epididymal fat of Ames dwarf mice

Gene expression analysis revealed an upregulation in the expression of IR ($p = 0.0209$), IRS-1 ($p = 0.0221$) and PGC1a ($p = 0.0033$) and a decrease in the gene expression of TNF-a ($p = 0.0114$) in the epididymal fat depot of df/df mice.

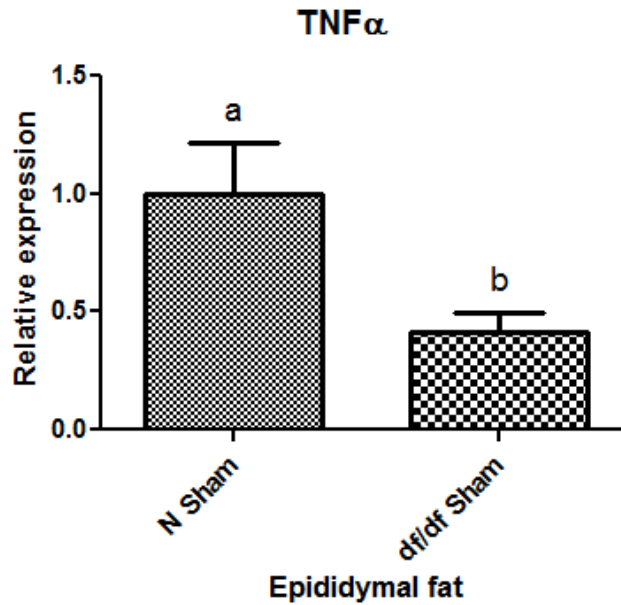


Figure 20: Ames dwarf mice show a downregulation in the expression of TNF α transcript in epididymal fat

3.8 Adiponectin and IL-6 protein levels in the Ames dwarf mouse

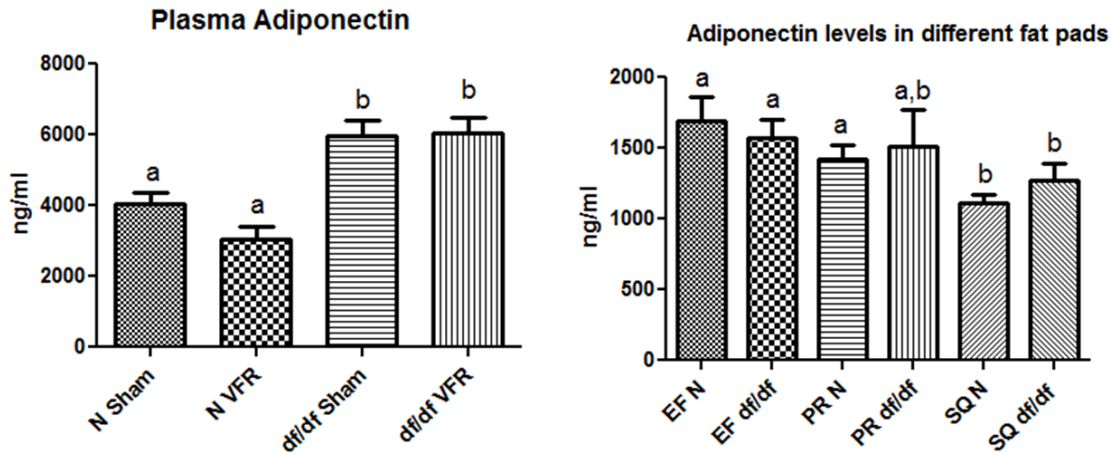


Figure 21: Adiponectin levels in circulation and in different fat pads

The level of adiponectin in circulation was significantly higher in df/df mice compared to N mice ($p = 0.0031$), although VFR had no difference on plasma levels of this adipokine either group of mice. Analysis of the adiponectin levels in different fat pads of N and df/df mice (~1 year old) revealed no differences in the different fat depots between the two groups of mice. However, EF and PR fat showed high levels of adiponectin compared to SQ fat depot in N mice ($p = 0.0038$ and $p = 0.0139$ respectively). Also, EF in df/df mice had higher expression of adiponectin compared to SQ fat depot of the mutant mice ($p = 0.0489$).

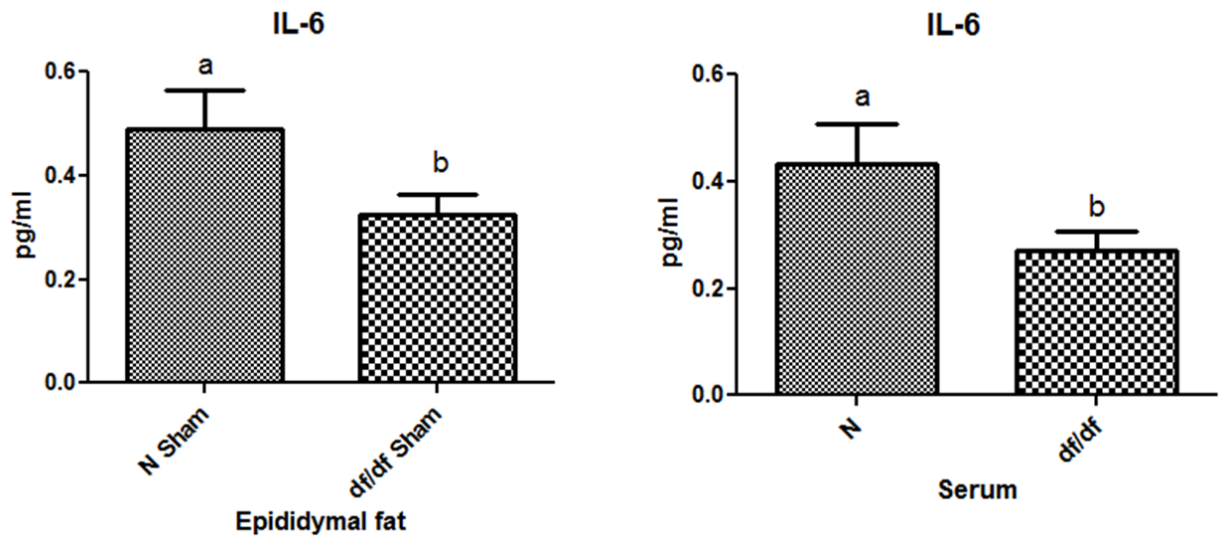


Figure 22: IL-6 protein levels in EF and serum

Protein levels of IL-6 were significantly low in the EF depot ($p = 0.0308$) of *df/df* mice. Bio-plex analysis of serum from N and *df/df* mice revealed a much lower level of IL-6 in circulation in the mutant dwarfs ($p = 0.0495$).

CHAPTER 4: DISCUSSION

Ames dwarf and GHRKO mice share similar phenotypic characteristics, such as extended longevity and healthspan and enhanced insulin sensitivity. The idea that fat developed in the absence of GH has beneficial effects was strengthened by visceral fat removal (VFR) experiments in GHRKO mice [69]. This intervention led to an improvement of insulin sensitivity in N mice with opposite effects in GHRKO mice.

The fact that *df/df* mice tend to become obese as they age, yet live longer and healthier lives compared to their wild-type siblings being very insulin sensitive with low circulating insulin and glucose levels and maintaining high plasma levels of anti-inflammatory adiponectin and low circulating levels of pro-inflammatory adipokines like IL-6, leads us to believe that the VF in these mutant dwarfs has a differential function than the same fat depots in N mice and does not negatively affect insulin signaling in these dwarfs.

The mice at the time of surgery were 3-6 months old. Thus, the percentage of VF removed (epididymal and perirenal fat depots) was lower in the *df/df* compared to the N mice. However, this percentage would be expected to increase in the mutant dwarfs with age due to their propensity to gain weight with age.

Surgically removing VF depots improved glucose tolerance only in N mice as seen by GTT. Moreover, GTT and ITT indicated that Ames dwarf mice showed improved glucose tolerance and insulin sensitivity compared to the controls, which supports previous data [2]. Although ITT did not show any significant effect on insulin sensitivity upon VFR in either group of mice, the HOMA score (calculated by the formula $(\text{insulin} \times \text{glucose})/22.5$), which is a measure of insulin sensitivity, with lower values corresponding to increased insulin

sensitivity, indicated that VFR improved insulin sensitivity only in the control mice leading to significantly decreased plasma insulin levels. Also, in parallel with ITT results, HOMA analysis indicated that df/df mice were much more insulin sensitive than the controls. The decrease in plasma insulin levels seen in the N VFR group was not accompanied by a change in glucose levels. This suggests that the decreased levels of insulin upon fat removal are sufficient to maintain euglycemic levels in the controls. However, in df/df mice, this surgical intervention led to an increase in plasma glucose concentration with no change in the level of secreted insulin. It is well known that skeletal muscle and adipose tissue are the major insulin-responsive organs. Moreover, removal of VF lead to an upregulation of GLUT4 mRNA in skeletal muscle of N mice, but a downregulation of this glucose transporter in the subcutaneous fat of df/df mice. This decreased expression of GLUT4 in SQ fat and the absence of functionally beneficial VF (due to VFR) in the mutants could probably lead to decreased glucose disposal and a corresponding increase in plasma glucose.

Analysis of gene expression in skeletal muscle revealed that VFR could have beneficial effects on insulin signaling only in N mice with no significant changes in gene expression in df/df mice. The upregulation of insulin receptor (IR), insulin receptor substrate-2 (IRS-2), phosphoinositide 3-kinase (PI3K), Akt 2 and GLUT4 transcript levels in the skeletal muscle of the control mice with visceral fat removed probably contribute to the increased insulin sensitivity seen in these mice.

Peroxisome proliferator-activated receptors (PPARs) are ligand-dependent transcription factors activated by different ligands such as fatty acids and thiazolidinediones (TZDs). Once activated, these nuclear receptors form heterodimers with retinoid X receptors (RXRs) and

bind to specific peroxisome proliferator response elements (PPREs) in the enhancers of target genes leading to activation of transcription of these genes [70]. Although highly expressed in white adipose tissue, several insulin-sensitive tissues express PPAR γ . Skeletal muscle PPAR γ increases glucose uptake and utilization. However, optimum expression and activation of PPAR γ seem to play an important role in maintaining whole-body insulin sensitivity. Muscle-specific PPAR γ knockout mice exhibit an increase in adiposity and develop insulin resistance; but are still responsive to TZDs [71]. On the other hand, in skeletal muscle of GHRKO mice, CR (which improves insulin sensitivity) led to a decrease in the expression of PPAR γ [70]. In our study, VFR caused an increase in the expression of PPAR γ as well as its coactivator (PGC1 α) at the mRNA level in skeletal muscle of mice only in the N VFR group. Thus, higher PPAR γ expression in the skeletal muscle seems to play a role in improving whole-body insulin sensitivity as seen with this surgical intervention in the control mice. The decreased insulin sensitivity seen in df/df mice upon VFR is probably not mediated by PPAR γ and PGC1 α expression in the skeletal muscle.

The expression and activation of Akt in skeletal muscle was checked by Western blot. Total Akt levels were higher in the df/df mice compared to the controls under insulin-stimulated as well as unstimulated states. Surprisingly, Akt activation, as determined by phosphorylation levels at S473 and T308, was highest in animals in the df/df VFR group upon insulin stimulation. The ratio of Akt (phosphorylated) to total Akt also revealed highest activation of Akt in the insulin-stimulated df/df mice with visceral fat removed. This would mean that, insulin activates the pathway to a much higher degree in the df/df mice with VF removed compared to the other animal groups. However, VFR does not have any beneficial

effects on whole-body insulin sensitivity in the *df/df* mice. Thus, it could be possible that this extent of pathway activation does not contribute positively to insulin signaling in the mutant mice. On the other hand, ‘hyperactivation’ of Akt could lead to disease conditions due to its known role in cell survival and proliferation. However, further studies would have to be carried out to understand the cause and consequences of Akt activation upon fat removal in these dwarf mice under insulin-stimulated conditions.

The effect of VFR on SQ fat was studied by analyzing the expression of genes involved in insulin signaling in this fat depot. The decrease in transcript levels of IR, IRS-1, PI3K, Akt 2 and GLUT4 in SQ fat of *df/df* mice in the VFR category may, in part, contribute to the loss of insulin sensitivity seen in these mice. Mice with adipose-specific knock out of PGC1 α are characterized by insulin resistance when fed a high-fat diet [72], demonstrating its role in maintaining insulin sensitivity. Ames dwarf mice in the VFR group showed a decrease in the expression of PGC1 α in SQ fat. Though there was no significant change in the gene expression of PPAR γ in this fat depot of *df/df* VFR mice, the lower transcript levels of PGC1 α might explain the decreased insulin sensitivity of the mice in this group. Ames dwarf mice in the sham-operated groups showed an increase in gene expression of IR and IRS-1 compared to N sham operated mice, which could explain, at least in part, the enhanced insulin sensitivity of the mutants.

Since hepatic IGF-1, under the action of GH, is the primary source of circulating IGF-1, *df/df* mice have very low levels of IGF-1 in circulation. However, qPCR analysis indicated an expression of IGF-1 in skeletal muscle, pituitary, SQ fat and EF. This locally expressed IGF-1 probably acts in an autocrine/paracrine manner. Also, VFR led to a decrease in IGF-1

transcript level in SQ fat of df/df mice, indicating cross-talk between VF and SQ fat. This surgical intervention did not lead to any change in the insulin sensitivity of df/df mice. Thus, decreased IGF-1 expression in SQ fat may not contribute to overall insulin sensitivity of these animals. The mechanisms underlying the interaction between the various fat depots would need further investigation.

To understand the correlation between VF and increased sensitivity of the df/df mice to insulin, we analyzed the gene expression of players involved in the insulin signaling pathway in EF of df/df and N mice in the sham-operated groups. There was an increase in the mRNA levels of IR, IRS-1 and PGC1 α in this VF depot of df/df mice only. Moreover, the expression of TNF α at the mRNA level was significantly lower in df/df EF relative to this fat depot of N mice. Ames dwarf mice also had lower levels of IL-6 protein in EF as well as in circulation, as revealed by Bio-plex analysis of this fat pad and serum from df/df and N mice. Moreover, protein levels of adiponectin were higher in EF compared to SQ fat of df/df mice. As expected, circulating adiponectin levels were higher in df/df mice compared to N mice; although VFR did not have any effect on these levels. One possible explanation for the lack of alteration in adiponectin levels in the mice upon VFR is that the removal of EF and PR fat depots causes a switch in the secretion of adiponectin by intact SQ fat as a compensatory mechanism. All these findings indicate the contribution of EF to positive insulin signaling in df/df mice. Analysis of the different fat pads from df/df and N mice, by ELISA, did not show any differences between the major VF depots (EF and PR fat) or SQ fat between the two groups of mice. Also, EF and PR fat depots had a higher expression of adiponectin protein compared to SQ fat in the case of N mice. Several studies support the idea that VF

produces adiponectin and this intra-abdominal fat determines the level of adiponectin in circulation [73-75]. In our study, mice used for determining adiponectin levels in fat pads were healthy and non-obese. Thus, fat at different sites in these mice, functions ‘normally’ with no dysregulation in the secretion of adiponectin. However, obesity would lead to the different fat pads having a differential secretory profile, with VF producing more pro-inflammatory adipokines and decreased adiponectin.

In summary, as expected, df/df mice exhibited increased glucose tolerance and insulin sensitivity compared to the wild-type siblings. Surgical removal of VF increased glucose tolerance and insulin sensitivity only in N mice. This surgical intervention led to an upregulation of genes responsible for enhancing insulin sensitivity in the skeletal muscle of N mice only; but led to a decreased expression of these genes in the SQ fat of df/df mice. The expression of total Akt, under insulin-stimulated and unstimulated conditions, was higher in the skeletal muscle of df/df mice compared to the controls. For as yet unidentified reasons, VFR led to the highest level of Akt activation in the skeletal muscle of df/df mice when stimulated with insulin. Even though df/df mice have very low plasma levels of IGF-1, they show a local expression of IGF-1 in different tissues. The increased expression of IR, IRS-1 and PGC1 α and downregulation of TNF α transcript levels as well decreased IL-6 protein expression in the EF and in circulation and high EF and plasma levels of adiponectin in df/df compared to N mice contributes to the increased insulin sensitivity of these mice. Thus, disruption of the GH/IGF-1 axis seems to lead to a delayed rate of aging and thus an extension of longevity of df/df mice (figure 23).

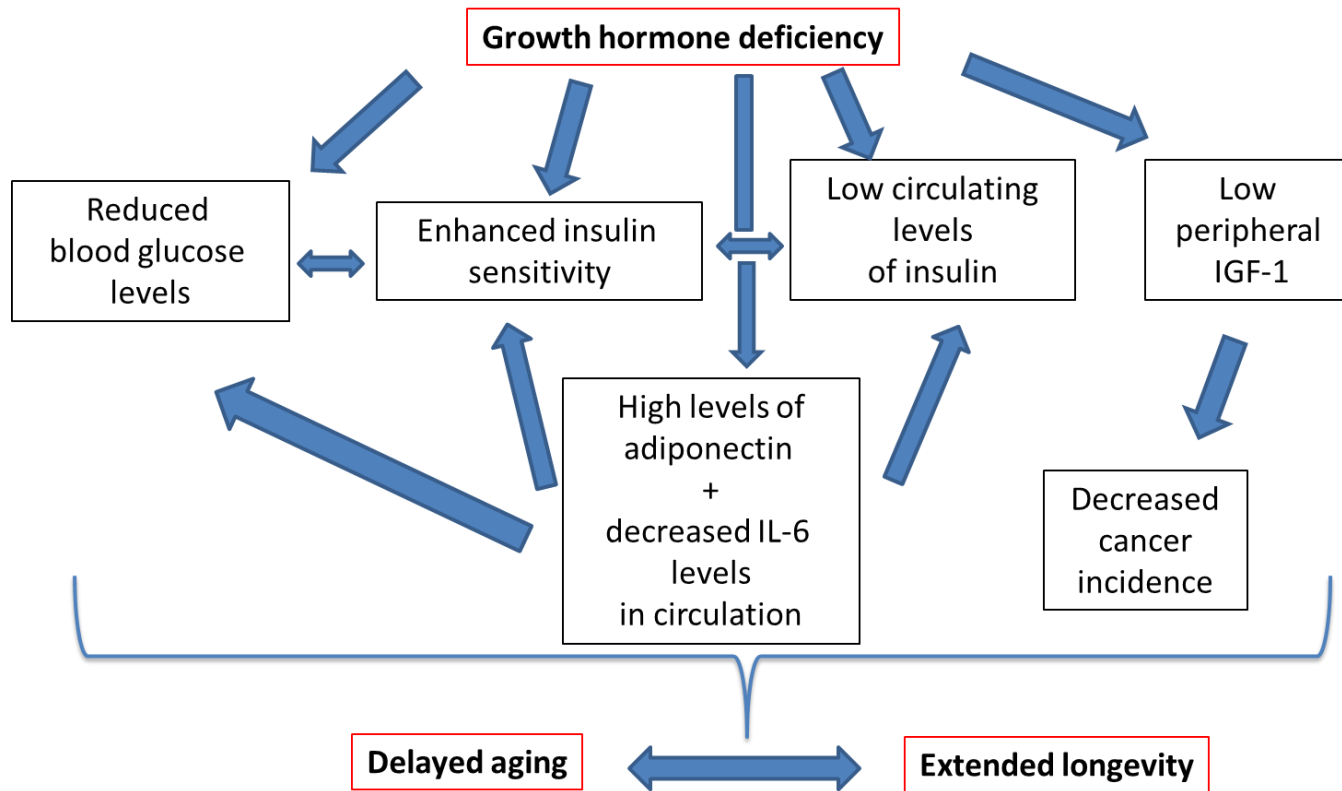


Figure 23: Proposed mechanisms of extended longevity in *df/df* mice

We conclude that VF developed in the absence of GH signaling has a differential secretory profile and altered gene expression that does not negatively affect insulin signaling in df/df mice and is not detrimental to the overall health of these mutants.

REFERENCES

1. Brown-Borg HM, B.K., Meliska CJ, Bartke A, *Dwarf mice and the ageing process*. Nature, 1996. **384**(6604): p. 33.
2. Bartke A, B.-B.H., Mattison J, Kinney B, Hauck S, Wright C., *Prolonged longevity of hypopituitary dwarf mice*. Exp Gerontol, 2001. **36**(1): p. 21-8.
3. Bartke A, B.M., Masternak M, *How diet interacts with longevity genes*. Hormones (Athens), 2008. **7**(1): p. 17-23.
4. Kinney BA, M.C., Steger RW, Bartke A, *Evidence that Ames dwarf mice age differently from their normal siblings in behavioral and learning and memory parameters*. Horm Behav, 2001. **39**(4): p. 277-84.
5. Ikeno Y, B.R., Hubbard GB, Lee S, Bartke A, *Delayed occurrence of fatal neoplastic diseases in ames dwarf mice: correlation to extended longevity*. J Gerontol A Biol Sci Med Sci, 2003. **58**(4): p. 291-6.
6. Bartke A, W.J., Mattison JA, Ingram DK, Miller RA, Roth GS, *Extending the lifespan of long-lived mice*. Nature, 2001. **414**(6862): p. 412.
7. Hassan M, L.N., Yacoub M, *Adipose tissue: friend or foe?* Nat Rev Cardiol, 2012. **9**(12): p. 689-702.
8. Nedergaard J, C.B., *The changed metabolic world with human brown adipose tissue: therapeutic visions*. Cell Metab, 2010. **11**(4): p. 268-72.
9. Rytka JM, W.S., Schoenle EJ, Konrad D., *The portal theory supported by venous drainage-selective fat transplantation*. Diabetes, 2011. **60**(1): p. 56-63.

10. Fontana L, E.J., Trujillo ME, Scherer PE, Klein S, *Visceral fat adipokine secretion is associated with systemic inflammation in obese humans*. Diabetes, 2007. **56**(4): p. 1010-3.
11. MM, I., *Subcutaneous and visceral adipose tissue: structural and functional differences*. Obes Rev, 2010. **11**(1): p. 11-8.
12. Tran TT, Y.Y., Gesta S, Kahn CR, *Beneficial effects of subcutaneous fat transplantation on metabolism*. Cell Metab, 2008. **7**(5): p. 410-20.
13. Omodei D, F.L., *Calorie restriction and prevention of age-associated chronic disease*. FEBS Lett, 2011. **585**(11): p. 1537-42.
14. Bartke A, W.R., *Metabolic characteristics of long-lived mice*. Front Genet, 2012. **3**.
15. Barzilai N, G.I., *The role of fat depletion in the biological benefits of caloric restriction*. J Nutr, 2001. **131**(3): p. 903S-906S.
16. Barzilai N, S.L., Liu BQ, Vuguin P, Cohen P, Wang J, Rossetti L, *Surgical removal of visceral fat reverses hepatic insulin resistance*. Diabetes, 1999. **48**(1): p. 94-8.
17. Kim YW, K.J., Lee SK, *Surgical removal of visceral fat decreases plasma free fatty acid and increases insulin sensitivity on liver and peripheral tissue in monosodium glutamate (MSG)-obese rats*. J Korean Med Sci., 1999. **14**(5): p. 539-45.
18. Gabriely I, M.X., Yang XM, Atzmon G, Rajala MW, Berg AH, Scherer P, Rossetti L, Barzilai N, *Removal of visceral fat prevents insulin resistance and glucose intolerance of aging: an adipokine-mediated process?* Diabetes, 2002. **51**(10): p. 2951-8.

19. Lottati M, K.C., Stefanovski D, Kirkman EL, Bergman RN, *Greater omentectomy improves insulin sensitivity in nonobese dogs*. Obesity (Silver Spring), 2009. **17**(4): p. 674-80.
20. Thörne A, L.F., Apelman J, Hellers G, Arner P, *A pilot study of long-term effects of a novel obesity treatment: omentectomy in connection with adjustable gastric banding*. Int J Obes Relat Metab Disord, 2002. **26**(2): p. 193-9.
21. Csendes A, M.F., Burgos AM, *A prospective randomized study comparing patients with morbid obesity submitted to laparotomic gastric bypass with or without omentectomy*. Obes Surg, 2009. **19**(4): p. 490-4.
22. Fabbrini E, T.R., Magkos F, Marks-Shulman PA, Eckhauser AW, Richards WO, Klein S, Abumrad NN, *Surgical removal of omental fat does not improve insulin sensitivity and cardiovascular risk factors in obese adults*. Gastroenterology, 2010. **139**(2): p. 448-55.
23. Hirashita T, O.M., Endo Y, Masuda T, Iwashita Y, Kitano S, *Effects of visceral fat resection and gastric banding in an obese diabetic rat model*. Surgery, 2012. **151**(1): p. 6-12.
24. Coelho M, O.T., Fernandes R, *Biochemistry of adipose tissue: an endocrine organ*. Arch Med Sci, 2013. **9**(2): p. 191-200.
25. Kern PA, D.G.G., Lu T, Rassouli N, Ranganathan G, *Adiponectin expression from human adipose tissue: relation to obesity, insulin resistance, and tumor necrosis factor-alpha expression*. Diabetes, 2003. **52**(7): p. 1779-85.

26. El-Wakkad A, H.N.-M., Sibaii H, El-Zayat SR, *Proinflammatory, anti-inflammatory cytokines and adipokines in students with central obesity*. *Cytokine*, 2013. **61**(2): p. 682-7.
27. Hu E, L.P., Spiegelman BM, *AdipoQ is a novel adipose-specific gene dysregulated in obesity*. *J Biol Chem*, 1996. **271**(18): p. 10697-703.
28. Kern PA, R.S., Li C, Wood L, Ranganathan G, *Adipose tissue tumor necrosis factor and interleukin-6 expression in human obesity and insulin resistance*. *Am J Physiol Endocrinol Metab*, 2001. **280**(5): p. E745-51.
29. Yang WS, L.W., Funahashi T, Tanaka S, Matsuzawa Y, Chao CL, Chen CL, Tai TY, Chuang LM., *Weight reduction increases plasma levels of an adipose-derived anti-inflammatory protein, adiponectin*. *J Clin Endocrinol Metab*, 2001. **86**(8): p. 3815-9.
30. Esposito K, P.A., Di Palo C, Giugliano G, Masella M, Marfella R, Giugliano D, *Effect of weight loss and lifestyle changes on vascular inflammatory markers in obese women: a randomized trial*. *JAMA*, 2003. **289**(14): p. 1799-904.
31. Lee KY, K.H., Shin YA, *Exercise improves adiponectin concentrations irrespective of the adiponectin gene polymorphisms SNP45 and the SNP276 in obese Korean women*. *Gene*, 2013. **516**(2): p. 271-6.
32. Ziccardi P, N.F., Giugliano G, Esposito K, Marfella R, Cioffi M, D'Andrea F, Molinari AM, Giugliano D, *Reduction of inflammatory cytokine concentrations and improvement of endothelial functions in obese women after weight loss over one year*. *Circulation*, 2002. **105**(7): p. 804-9.

33. Yadav A, K.M., Saini V, Yadav A, *Role of leptin and adiponectin in insulin resistance*. Clin Chim Acta, 2013. **417**: p. 80-4.
34. Masternak MM, B.A., *Growth hormone, inflammation and aging*. Pathobiol Aging Age Relat Dis, 2012. **2**.
35. Yamauchi T, K.J., Waki H, Terauchi Y, Kubota N, Hara K, Mori Y, Ide T, Murakami K, Tsuboyama-Kasaoka N, Ezaki O, Akanuma Y, Gavrilova O, Vinson C, Reitman ML, Kagechika H, Shudo K, Yoda M, Nakano Y, Tobe K, Nagai R, Kimura S, Tomita M, Froguel P, Kadowaki T, *The fat-derived hormone adiponectin reverses insulin resistance associated with both lipoatrophy and obesity*. Nat Med, 2001. **7**(8): p. 941-6.
36. Berg AH, C.T., Du X, Brownlee M, Scherer PE, *The adipocyte-secreted protein Acrp30 enhances hepatic insulin action*. Nat Med, 2001. **7**(8): p. 947-53.
37. Ogden CL, C.M., Kit BK, Flegal KM, *Prevalence of obesity in the United States, 2009-2010*. NCHS Data Brief, 2012. **82**: p. 1-8.
38. French SA, S.M., Jeffery RW, *Environmental influences on eating and physical activity*. Annu Rev Public Health, 2001. **22**: p. 309-35.
39. Du H, B.D., Li L, Whitlock G, Guo Y, Collins R, Chen J, Bian Z, Hong LS, Feng S, Chen X, Chen L, Zhou R, Mao E, Peto R, Chen Z; China Kadoorie Biobank Collaborative Group, *Physical activity and sedentary leisure time and their associations with BMI, waist circumference, and percentage body fat in 0.5 million adults: the China Kadoorie Biobank study*. Am J Clin Nutr, 2013. **97**(3): p. 487-96.

40. Curat CA, W.V., Sengenès C, Miranville A, Tonus C, Busse R, Bouloumié A, *Macrophages in human visceral adipose tissue: increased accumulation in obesity and a source of resistin and visfatin*. Diabetologia, 2006. **49**(4): p. 744-7.
41. J, P., *Monocyte Chemoattractant Protein 1 (MCP-1) in obesity and diabetes*. Cytokine, 2012. **60**(1): p. 1-12.
42. Kanda H, T.S., Tamori Y, Kotani K, Hiasa K, Kitazawa R, Kitazawa S, Miyachi H, Maeda S, Egashira K, Kasuga M, *MCP-1 contributes to macrophage infiltration into adipose tissue, insulin resistance, and hepatic steatosis in obesity*. J Clin Invest, 2006. **116**(6): p. 1494-505.
43. Lumeng CN, B.J., Saltiel AR, *Obesity induces a phenotypic switch in adipose tissue macrophage polarization*. J Clin Invest, 2007. **117**(1): p. 175-84.
44. Lumeng CN, D.J., Westcott DJ, Saltiel AR, *Phenotypic switching of adipose tissue macrophages with obesity is generated by spatiotemporal differences in macrophage subtypes*. Diabetes, 2008. **57**(12): p. 3239-46.
45. Association, A.D., *Diagnosis and classification of diabetes mellitus*. Diabetes Care, 2004: p. S5-S10.
46. Kahn BB, F.J., *Obesity and insulin resistance*. J Clin Invest, 2000. **106**(4): p. 473-81.
47. Aballay LR, E.A., Díaz Mdel P, Navarro A, Muñoz SE, *Overweight and obesity: a review of their relationship to metabolic syndrome, cardiovascular disease, and cancer in South America*. Nutr Rev, 2013. **71**(3): p. 168-79.
48. Smyth S, H.A., *Diabetes and obesity: the twin epidemics*. Nat Med, 2006. **12**(1): p. 75-80.

49. H, H., *The mode of action of thiazolidinediones*. Diabetes Metab Res Rev, 2002: p. S10-5.
50. Erdmann E, C.B., Wilcox RG, Skene AM, Massi-Benedetti M, Yates J, Tan M, Spanheimer R, Standl E, Dormandy JA; PROactive investigators, *Pioglitazone use and heart failure in patients with type 2 diabetes and preexisting cardiovascular disease: data from the PROactive study (PROactive 08)*. Diabetes Care, 2007. **30**(11): p. 2773-8.
51. Lecka-Czernik, B., *Bone Loss in Diabetes: Use of Antidiabetic Thiazolidinediones and Secondary Osteoporosis*. Curr Osteoporos Rep, 2010. **8**(4): p. 178-184.
52. AJ, S., *Hepatotoxicity with thiazolidinediones: is it a class effect?* Drug Saf, 2001. **24**(12): p. 873-88.
53. Saltiel AR, K.C., *Insulin signalling and the regulation of glucose and lipid metabolism*. Nature, 2001. **414**(6865): p. 799-806.
54. Lizcano JM, A.D., *The insulin signalling pathway*. Curr Biol, 2002. **12**(7): p. R236-8.
55. Leto D, S.A., *Regulation of glucose transport by insulin: traffic control of GLUT4*. Nat Rev Mol Cell Biol, 2012. **13**(6): p. 383-96.
56. Longo VD, F.C., *Evolutionary medicine: from dwarf model systems to healthy centenarians?* Science, 2003. **299**(5611): p. 1342-6.
57. Holzenberger M, D.J., Ducos B, Leneuve P, Géloën A, Even PC, Cervera P, Le Bouc Y, *IGF-1 receptor regulates lifespan and resistance to oxidative stress in mice*. Nature, 2003. **421**(6919): p. 182-7.

58. Dominici FP, H.S., Argentino DP, Bartke A, Turyn D, *Increased insulin sensitivity and upregulation of insulin receptor, insulin receptor substrate (IRS)-1 and IRS-2 in liver of Ames dwarf mice.* J Endocrinol, 2002. **173**(1): p. 81-94.
59. Zhou Y, X.B., Maheshwari HG, He L, Reed M, Lozykowski M, Okada S, Cataldo L, Coschigamo K, Wagner TE, Baumann G, Kopchick JJ, *A mammalian model for Laron syndrome produced by targeted disruption of the mouse growth hormone receptor/binding protein gene (the Laron mouse).* Proc Natl Acad Sci U S A, 1997. **94**(24): p. 13215-20.
60. Dominici FP, A.D.G., Bartke A, Kopchick JJ, Turyn D, *Compensatory alterations of insulin signal transduction in liver of growth hormone receptor knockout mice.* J Endocrinol, 2000. **166**(3): p. 579-90.
61. Ikeno Y, H.G., Lee S, Cortez LA, Lew CM, Webb CR, Berryman DE, List EO, Kopchick JJ, Bartke A, *Reduced incidence and delayed occurrence of fatal neoplastic diseases in growth hormone receptor/binding protein knockout mice.* J Gerontol A Biol Sci Med Sci, 2009. **64**(5): p. 522-9.
62. Guevara-Aguirre J, B.P., Guevara-Aguirre M, Wei M, Madia F, Cheng CW, Hwang D, Martin-Montalvo A, Saavedra J, Ingles S, de Cabo R, Cohen P, Longo VD, *Growth hormone receptor deficiency is associated with a major reduction in pro-aging signaling, cancer, and diabetes in humans.* Sci Transl Med, 2011. **3**(70): p. 70ra13.
63. Rosenbloom AL, G.-A.J., Rosenfeld RG, Francke U, *Growth hormone receptor deficiency in Ecuador.* J Clin Endocrinol Metab, 1999. **84**(12): p. 4436-43.

64. Bartke A, C.V., Bailey B, Zaczek D, Turyn D, *Consequences of growth hormone (GH) overexpression and GH resistance*. *Neuropeptides*, 2002. **36**(2-3): p. 201-8.
65. Wasada T, A.K., Sato A, Katsumori K, Muto K, Tomonaga O, Yokoyama H, Iwasaki N, Babazono T, Takahashi C, Iwamoto Y, Omori Y, Hizuka N, *Assessment of insulin resistance in acromegaly associated with diabetes mellitus before and after transsphenoidal adenomectomy*. *Endocr J*, 1997. **44**(4): p. 617-20.
66. Panici JA, H.J., Miller RA, Bartke A, Spong A, Masternak MM, *Early life growth hormone treatment shortens longevity and decreases cellular stress resistance in long-lived mutant mice*. *FASEB J*, 2010. **24**(12): p. 5073-9.
67. Masternak MM, P.J., Wang F, Wang Z, Spong A, *The effects of growth hormone (GH) treatment on GH and insulin/IGF-1 signaling in long-lived Ames dwarf mice*. *J Gerontol A Biol Sci Med Sci*, 2010. **65**(1): p. 24-30.
68. Masternak MM, P.J., Bonkowski MS, Hughes LF, Bartke A, *Insulin sensitivity as a key mediator of growth hormone actions on longevity*. *J Gerontol A Biol Sci Med Sci*, 2009. **64**(5): p. 516-21.
69. Masternak MM, B.A., Wang F, Spong A, Gesing A, Fang Y, Salmon AB, Hughes LF, Liberati T, Boparai R, Kopchick JJ, Westbrook R, *Metabolic effects of intra-abdominal fat in GHRKO mice*. *Aging Cell*, 2012. **11**(1): p. 73-81.
70. Masternak MM, B.A., *PPARs in Calorie Restricted and Genetically Long-Lived Mice*. *PPAR Res*, 2007. **2007**.
71. Norris AW, C.L., Fisher SJ, Szanto I, Ristow M, Jozsi AC, Hirshman MF, Rosen ED, Goodyear LJ, Gonzalez FJ, Spiegelman BM, Kahn CR, *Muscle-specific PPARgamma-*

- deficient mice develop increased adiposity and insulin resistance but respond to thiazolidinediones.* J Clin Invest, 2003. **112**(4): p. 608-18.
72. Kleiner S, M.R., Laznik D, Ye L, Jurczak MJ, Jornayvaz FR, Estall JL, Chatterjee Bhowmick D, Shulman GI, Spiegelman BM, *Development of insulin resistance in mice lacking PGC-1 α in adipose tissues.* Proc Natl Acad Sci U S A, 2012. **109**(24): p. 9635-40.
73. Halleux CM, T.M., Delporte ML, Detry R, Funahashi T, Matsuzawa Y, Brichard SM, *Secretion of adiponectin and regulation of apM1 gene expression in human visceral adipose tissue.* Biochem Biophys Res Commun, 2001. **288**(5): p. 1102-7.
74. Motoshima H, W.X., Sinha MK, Hardy VE, Rosato EL, Barbot DJ, Rosato FE, Goldstein BJ, *Differential regulation of adiponectin secretion from cultured human omental and subcutaneous adipocytes: effects of insulin and rosiglitazone.* J Clin Endocrinol Metab, 2002. **87**(12): p. 5662-7.
75. Cnop M, H.P., Utzschneider KM, Carr DB, Sinha MK, Boyko EJ, Retzlaff BM, Knopp RH, Brunzell JD, Kahn SE, *Relationship of adiponectin to body fat distribution, insulin sensitivity and plasma lipoproteins: evidence for independent roles of age and sex.* Diabetologia, 2003. **46**(4): p. 459-69.